

May 17, 2016

Dear Editor,

We have received the comments from the two reviewers of the manuscript. Below are our responses and the revisions that we have made in the manuscript.

Thank you for your efforts on this manuscript. We look forward to hearing from you.

Best Regards,

Xuexi Tie

Response to Referee #1

We thank the Referee for the careful reading of the manuscript and helpful comments. According to the suggestions of the referee, the comments have been carefully addressed, and the paper is carefully revised. We believe that the revised paper has been significantly improved after addressing the comments of the referee. We respond to each specific comment below. The original comments by the Referee are shown in bold italics. Our reply is shown in blue.

General comments:

1. The paper by Long X. et al. assesses the impact of crop field burning (CFB) and topography on air quality in North China Plain. The contribution of crop field burning is quantified. This analysis would have a substantial impact on policy.

We thank the referee for the careful reading and the valuable comments that helped improving our paper.

2. However, I think the impact of CFB and mountainous topography are two distinct impact sources. Please justify the reason to address these two distinct impacts in this single study.

We thank the referee for the thoughtful comment. We added these two impacts together because these two effects are related to each other by the following reasons.

- a. One goal of the study is to analyze the effect of CFB on aerosol pollution in the northern NCP (NNCP), where the capital city of China (Beijing) locates. Whereas the major CFB occurred in the southern NCP (SNCP). As shown in the analysis, with the prevailing southerly winds, the regional transport plays important roles to transport CFB pollutants from SNCP to NNCP.
- b. As shown by the measurements, the mountains play important roles for the northward transport, and cause the accumulation of the aerosol pollutants at the foothill of the mountains. By considering the above reasons, it is important to add these two important effects together in the analysis. We added some statements in the revised paper.

Line 99-104, “Thereafter we analyzed the regional transport of CFB emissions from

SNCP to NNCP driven by prevailing southerly winds. Under the continuously southerly wind condition, the mountains play important roles for the northward transport, and cause the accumulation of the aerosol pollutants at the foothill of the mountains. We also analyzed the impact of mountains (especially the Taihang Mountains and the Yanshan Mountains) on the air pollution transport.”

Line 147-149, “Considering the continuously southerly winds and the topographic conditions, we studied the impact of the mountains on the air pollution transport.”

Line 351-355, “Indeed, the CFB pollution plume go through a long-range transport to NNCP can cause an obvious increase to PM_{2.5} concentration, with the maximum daily average contribution of 32% (Table 5). Such a high transported contribution indicates that the CFB is not only one of the significant local pollution sources, but also a considerable regional pollution source.”

Detailed Comments

1. Introduction. Page 3 Line 17, “. . . it is lack of study for the quantitative effect . . .” I do not think it is appropriate to claim this without justification. A number of source apportionment studies have quantified the contribution of biomass burning in Beijing with modeling approach^{1,2,3}. A more comprehensive review of previous studies should be summarized in this part.

To response the Referee’s comments, we modified and added a summary of previous studies.

Line 59-67, “Numerous studies have quantified the contribution of biomass burning and CFB to PM pollution in China. According to Yao et al. (2016), Cheng et al. (2013), Wang et al. (2009; 2007) and Song et al. (2007), biomass burning has important impacts on the ambient PM_{2.5} concentrations (15-24% in Beijing and 4-19% in Guangzhou). Yan et al. (2010) captured a heavy pollution with PM₁₀ concentrations higher than 350 $\mu\text{g m}^{-3}$ in some CFB locations. It is reported that CFB may contribute more than 30% of the PM₁₀ increase during CFB incidents (Zhu et al., 2012; Zha et al. 2013; Su et al., 2012). Cheng et al. (2014) report a summer case that CFB contributed 37% of PM_{2.5} concentrations in the Yangtze River delta.”

Line 67-75, “The impact of CFB to air quality is continental and regional. Air quality in China is influenced by the CFB occurred in Southeast Asia and on the Indian Peninsula (Qin et al., 2006). Mukai et al. (2014) have reported that CFB emissions in Southeast Asia contribute the carbonaceous aerosols in Beijing. Within China, the inter-province

transported air pollutants emitted from CFB significantly affect regional PM levels and air quality (Cheng et al., 2014;Zhu et al., 2012). For Beijing, the smoke particles from CFB are expected to be one of the major components (Wang et al., 2014;Cheng et al., 2013), though the percentage of transported sources are seldom specified (Zhang et al., 2016).”

2. It should be also noted in the manuscript on what the novelty of this study is.

Thanks. The novelty of this study is to use multiply methods to quantify the impacts of a serious CFB incident on the aerosol pollution in regional scale. The main methods and conclusions include (1) using satellite data to generate the CFB emission inventory with higher temporal and spatial resolution, (2) using WRF-CHEM model to study the regional transport from the burning region (SNCP) to the NNCP (where the capital city of Beijing locates), and (3) quantifying the effect of the mountains on the accumulation of pollutants at the foothill of the mountains. The combination of the multiply methods provides a better understanding of the effect of CFB on the regional air pollution. We modified and added explicit statements in the revised paper.

Line 32-34, “This study suggests that the prohibition of CFB should be strict not just in or around Beijing, but also on the ulterior crop growth areas of SNCP.”

Line 449-456, “In recent years, the NCP region, including the capital city of Beijing, has been suffering serious haze pollution problem, especially in winter and summer. Most studies concerned about the intense secondary formation, huge regional transport of pollutants, stationary meteorological conditions and large local emission. In autumn, CFB and movement of wind based on large scale topography are important in NCP, whereas the percentage of transported CFB emission sources are seldom specified. This is probably resulted from the contingency of CFB activities during harvest period and the limitation of temporal resolution of CFB emission inventories.”

Line 464-467, “A more detailed CFB emission inventory was generated in NCP. The daily CFB emissions were estimated depending on CFB activities captured by MODIS. Plenty of pollutants emitted from SNCP on Oct. 6th and 7th, producing plenty of PM_{2.5} pollution, but few in NNCP during the entire haze period.”

Line 486-496, “Another major finding is that the mountains, surrounding the NCP in the north and west, play significant roles in enhancing the PM_{2.5} pollution in NNCP through the blocking effect. The mountains block and redirect the airflows, causing the pollution accumulation along the foothill of mountains. The Taihang Mountains had greater impacts on PM_{2.5} concentration than the Yanshan Mountains.

On account of various factors, such as pollutant long-range transport and pollutant accumulation caused by mountain effects, the prohibition of CFB should be strict not just in or around Beijing, but also on the ulterior crop growth areas of SNCP. Other PM_{2.5} emissions in the SNCP should be significantly limited in order to reduce the occurrences of heavy haze events in NNCP region, including the Beijing City.”

3. Also, Summary of references on biomass burning emissions and the influence of mountains in NCP on air pollution is needed in introduction part as well.

- a. A comprehensive summary of biomass burning emission has been added in the revised paper.

Line 39-48, “Crop residue resources in China rank the first in the world, accounting for 17.3% of the global production (Bi et al., 2010), and increasing with the average annual proportion of 4% (Hong et al., 2015;Zhao et al., 2010). Compared with other approaches, crop field burning (CFB) is the most effective and less expensive to remove residues. The national annual average proportion of CFB to total residues is about 11-25%(Cao et al., 2008;Hao and Liu, 1994;Streets et al., 2003;Wang and Zhang, 2008;Zhao et al., 2010). Large numbers of annual CFB occur in China (Zhang et al., 2015; Yan et al., 2006), especially during the post-harvest seasons (Zhang et al., 2016;Shi et al., 2014;Cao et al., 2008).”

Line 52-66, “However, CFB have adverse impacts on traffic conditions and ecology environments (Shi et al., 2014;Zhang, 2009), and release plenty of pollutants, such as CO, SO₂, VOC, NO_x and PM_{2.5} (Koppmann et al., 2005;Li et al., 2008). According to Guan et al. (2014) and Lu et al. (2011), annual CFB contribute about 13% of the total particulate matter (PM) emissions in China (Zhang et al., 2016). And it is more prominent during the harvest periods due to its strong seasonal dependence. Numerous studies have quantified the contribution of biomass burning and CFB to PM pollution in China. According to Yao et al. (2016), Cheng et al. (2013), Wang et al. (2009; 2007) and Song et al. (2007), biomass burning has important impacts on the ambient PM_{2.5} concentrations (15-24% in Beijing and 4-19% in Guangzhou). Yan et al. (2010) captured a heavy pollution with PM₁₀ concentrations higher than 350 $\mu\text{g m}^{-3}$ in some CFB locations. It is reported that CFB may contribute more than 30% of the PM₁₀ increase during CFB incidents (Zhu et al., 2012; Zha et al. 2013;Su et al., 2012). Cheng et al. (2014) report a summer case that CFB contributed 37% of PM_{2.5} concentrations in the Yangtze River delta.”

- b. We modified and added explicit statements of provincial CFB emission inventory processing in Line 192-197 and Line 210-221. And we updated the provincial statistical data and related results. The detailed results and related references were added in supplementary data of Table S1, Table S2 and Table S3.

Line 192-197, “This situation may be resulted from the limitation of local enforcement of regulation despite CFB have already been banned (Zhang and Cao, 2015;Shi et al., 2014). The CFB have a seasonal pattern due to the post-harvest activities with two distinct peaks in summer and autumn, especially in June (33-59%) and October (6-19%) (**Fig. 2b**). The strong seasonal dependence character suggests that the CFB emissions during October are much larger than annual averages.”

Line 210-221, “where i stands for each province and k for different crop species of rice, corn and wheat. $E_{i,co}$ stands for CO emission from CFB of i -th province in gigagrams

[Gg]. $P_{i,k}$ is the yield of crop in Gg. F_i is the proportion of residues burned in the field. D_k is the dry fraction of crop residue (dry matter). R_k is the residue-to-crop ratio (dry matter). CE_k is the combustion efficiency and EF_{co} is the emission factors of CFB. The $P_{i,k}$ values were taken from an official statistical yearbook (NBS, 2015) (**Table S1**), and the F_i on a provincial basis were taken from Wang and Zhang (2008) and Zhang Yisheng (Unpublished doctor thesis-in Chinese) (**Table S1**). The parameters of D_k , R_k , and CE_k are listed in **Table S2**. The EF_{co} from CFB was summarized range from 52 to 141 g kg⁻¹ in China (**Table S3**). In this study, we used 111 g kg⁻¹ as the average EF_{co} of crop residue, which was used to estimate the emissions from global open burning (Wiedinmyer et al., 2011).”

c. The influence of mountains in NCP on air pollution is added in **Introduction**.

Line 80-91, “Yanshan and Taihang Mountains surround the NCP in the north and west (**Fig. 1c**). Such topography affects air pollution though PBL in complex ways (Miao et al., 2015b;Sun et al., 2013;Liu et al., 2009). Hu et al. (2014) have reported that the Loess Plateau and NCP result in a mountain-plains solenoid circulation, exacerbating air pollution over NCP. Chen et al. (2009) have founded that a mountain chimney effect is dominated by mountain-valley breeze, enhancing the surface air pollution in Beijing. The mountain-plain breeze develops frequently in Beijing and may play important roles in modulating the local air quality (Miao et al., 2015b;Hu et al., 2014;Chen et al., 2009). Miao et al. (2015a) founded that the mountains played a significant role in the sea-land aerosol circulation and the pollutants could be transported and accumulated in the NCP areas along the mountains, which is treated as the blocking effect (Zhao et al., 2015).”

4. Further work on modeling evaluation and validation of model are needed. Page 5 Line 20 states that the aerosol module from CMAQv4.6, released in 2006 is used in this study. Could the authors explain why to choose version 4.6 instead the latest version of CMAQ? It has been accounted by Baek, et al. 4 that the simulated OM tends to be underestimated due to the uncertainty in secondary organic aerosols mechanism. However, Figure 4 shows that

simulated and observed PM2.5 mass concentration matches well. So is it possible to evaluate the model with PM2.5 species mass concentration and their precursor mass concentrations?

In order to response the referee's comments, we added several revisions. We believe that these revisions help to better evaluate the model result.

a. A more detailed model description was added in **Section 3.1 Model description**:

Line 153-160, "The specific version of WRF-CHEM model is developed by Li et al. (2010; 2011; 2012), with a new flexible gas phase chemical module and the CMAQ (version 4.6) aerosol module developed by US EPA (Binkowski and Roselle, 2003). The wet deposition follows the CMAQ method and the dry deposition is parameterized following Wesely (1989). The photolysis rates are calculated using the FTUV (Li et al., 2005; Tie et al., 2003), in which the impacts of aerosols and clouds on the photochemistry are considered (Li et al., 2011)."

Line 162-166, "Meanwhile, the ISORROPIA Version 1.7 (<http://nenes.eas.gatech.edu/ISORROPIA/>) is utilized to simulate the inorganic aerosols, which is primarily used to predict the thermodynamic equilibrium between the ammonia-sulfate-nitrate-chloride-water aerosols and their gas phase precursors of H₂SO₄-HNO₃-NH₃-HCl-water vapor."

Line 184-185, "The biogenic emissions are calculated on-line with the WRF-CHEM model using the MEGAN model (Guenther, 2006)."

b. The explanation of the statistical characteristics of the evaluation is added.

Line 272-280, “The simulations are overall lower than the observations with NMB of -12% in NNCP and -7% in SNCP. Considering the high average $\text{PM}_{2.5}$ concentration with $200.0 \mu\text{g m}^{-3}$ in NNCP and $184.1 \mu\text{g m}^{-3}$ in SNCP, obvious underestimates exist with the overall concentrations of $24.0 \mu\text{g m}^{-3}$ in NNCP and $12.9 \mu\text{g m}^{-3}$ in SNCP. This may be related to the CMAQ (version 4.6) aerosol module, which is likely to underestimated OM due to the uncertainty in secondary organic aerosols mechanism (Baek et al., 2011). Meanwhile, the underestimates are also related to the negative bias in S3, which may be related to cloud contamination (**Fig. S1**).”

- c. More evaluations of model calculation, such as NO_2 and O_3 , were added **in the Section 4.2 Statistical characteristics of the evaluation**. A new figure of the comparison between the calculated and measured NO_2 and O_3 is also added in the section (Fig. 4b and 4c), and related descriptions were modified.

Line 258-260, “In order to evaluate the model performance, the model simulations were compared with the measured results in both species concentrations ($\text{PM}_{2.5}$, O_3 and NO_2) and meteorological parameters (wind speed, wind direction and PBLH).”

Line 268-272, “**Figure 4** shows the measured and calculated temporal variations of regional average species concentrations, including $\text{PM}_{2.5}$, O_3 and NO_2 . The WRF-CHEM model reproduced the pollution episode well, with a good agreement with observations. The correlation coefficients (R) of simulated and measured $\text{PM}_{2.5}$ concentrations are 0.88 in both NNCP and SNCP (**Fig. 4a**).”

Line 281-283, “The simulations of O_3 and NO_2 are also agree well with observations, with R greater than 0.77 and absolute NMB lower than 17% (**Fig. 4b and 4c**)”

- d. Pattern comparisons of simulated vs. observed near-surface $\text{PM}_{2.5}$ concentrations were added

in Fig. 9 and Fig.10.

Line 370-372, “The pattern comparisons between simulated and observed near-surface $PM_{2.5}$ concentrations ($TPM_{2.5}$) perform well (**Fig. 9 Left Panels**).”

Line 767-770, “**Figure 9** ... Left panels also show the pattern comparisons of simulated vs. observed near-surface $PM_{2.5}$ concentrations ($TPM_{2.5}$), with $PM_{2.5}$ observations of colored circles. Black arrows denote simulated surface winds.”

Line 414-415, “exhibiting a good performance of the pattern comparisons between simulated and observed near-surface $PM_{2.5}$ concentrations.”

Line 771-775, “**Figure 10** The elevation contours and the pattern comparisons of simulated vs. observed near-surface $PM_{2.5}$ concentrations from 12:00 7th to 00:00 10th. Colored circles: $PM_{2.5}$ observations of foothill sites; Colored squares: $PM_{2.5}$ observations of non-foothill sites; Black arrows: simulated surface winds. The 200-meter contour was highlighted with bold black line.”

5. Page 9 Line 10 states that “strong southerly wind, with mean wind speed of 2.5 (2.7) m s⁻¹ in NNCP and 3.0 (3.6) m s⁻¹ in SNCP” to illustrate that “The pollution is continuously transported from SNCP to NNCP”. It’s not strong enough to get such conclusion. Trajectory analysis and wind speed profile analysis should be included.

According to the referee’s suggestions, we added a backward trajectory analysis and wind speed profile analysis in the **Section 4.3 Characteristics of the heavy pollution events**. A new figure of the backward trajectory analysis during S1 was added in the revised paper. As shown in Fig. 6, the prevailing wind during the analysis period (S1) is continuously from south to north.

Line 296-301, “The backward trajectories, with the HYSPLIT model online version, of

BJ, TJ and BD during S1 reflected how the CFB influenced the NNCP region (**Fig. 6**). The air mass mainly came from the south, originating from the SNCP region. The pollutants are continuously transported from SNCP to NNCP, leading to pollutants accumulation in NNCP...”

6. *In Section 4.5, it is written “The differences between the simulations with or without mountains showed the net effect of the topography on PM_{2.5} concentration”. I wonder if it is appropriate to make this assumption for several reasons. First, the impact of topography is complicated. I am not sure if it is good to represent it just as “reduced to the averaged altitude”. Second, the NCEP FNL Operational Global Analysis data is employed as the initial meteorological condition. It means the initial condition is “real” (with mountains) in all scenarios.*

- a. Thanks for the suggestion. As an online model, the reduction of the topography in WRF-CHEM can lead to dynamical changes, such as the wind speeds at the foothill of the mountains. We agree with the referee that there are some shortcomings of the method, and we modified the text to point out these shortcomings **in the Section. 4.5 Impact of mountains**.

Line 396-405, “In this study, we utilized the differences between the simulations with or without mountains to represent the effect of the topography on PM_{2.5} concentration, which were calculated based on Eq. (9). As an on-line dynamical model, the topography changes in WRF-CHEM can lead to dynamical changes, such as the wind speeds at the foothill of the mountains. This is a useful and traditional sensitivity analysis method for numerical model to quantify the mountains effects, but with some shortcomings, which are to bring uncertainties to the sensitivity experiment. Firstly, the impact of topography is complicated to be completely quantified only by the altitude remove behavior. Secondly, the initial NCEP FNL data with mountains is treated as “real” in scenarios without mountains.”

- b. The guiding effect is treated as part of the mountain blocking effect. We modified and added the description in the revised paper.

Line 31-34, "...through the blocking effect. The mountains block and redirect the airflows, causing the pollutant accumulations along the foothill of mountains. This study suggests that the prohibition of CFB should be strict not just in or around Beijing, but also on the ulterior crop growth areas of SNCP."

Line 418-423, "Here, it is attributed to the mountain blocking effect, which has two categories of influences. Firstly, the mountains block the airflows, causing pollutant accumulation and resulting in high PM_{2.5} loading at the foothill of mountains (Influence-1, block). Secondly, the mountains redirect the airflows, causing the pollutants move toward the downwind foothill areas (Influence-2, redirect)."

Line 486-491, "Another major finding is that the mountains, surrounding the NCP in the north and west, play significant roles in enhancing the PM_{2.5} pollution in NNCP through the blocking effect. Mountains block and redirect the airflows, causing the pollution accumulation along the foothill of mountains. The Taihang Mountains had greater impacts on PM_{2.5} concentration than the Yanshan Mountains."

Supplementary data of Fig. S3, "Fig. S3 The schematic pictures of mountains effect along with the topography of the NCP region. (a) Mountains block the airflows and cause pollutants accumulated at the foothill of mountains. (b) Mountains redirect the airflows, and cause pollutants move toward the downwind foothill areas (Influence-2, redirect)."

7. The spin-up time is only 12 hours. I think the spin- up time is not long enough to get balanced. Also I wonder if any nudging method is used in this study (it should be explained in method part). If so, the contribution might be changed due to the nudging. Third, the domain is not large enough to ignore the impacts of "real" boundary condition. The mountainous topography may change the large-scale circulation.

We rerun the model to extend the spin-up time to 3 days (Line 178), and updated related results (Line 442-444, Fig. 11...). As a regional model, the boundary effect cannot be avoided in the

WRF-CHEM. We agree with the referee that change model domain and use nudging method can change the model results. But we also need to consider the balance between large domain and cost of computation time. As a result, we have tested for different sizes for the model domains (900km x 900km). We think that the current domain 1200km x 1800km is reasonable and large enough for considering the lateral boundary effects. The important mountains (Taihang and Yanshan) have included in this domain.

Response to Referee #2

We thank the Referee for the careful reading of the manuscript and helpful comments. According to the suggestions of the referee, the comments have been carefully addressed, and the paper is carefully revised. We believe that the revised paper has been significantly improved after addressing the comments of the referee. We respond to each specific comment below. The original comments by the Referee are shown in bold italics. Our reply is shown in blue.

General comments:

- 1. This paper conducts a numerical study to investigate the impact of crop field burning and topography on haze pollution in the North China Plain. This is an interesting study and potentially will be useful for air quality management in this region. However, there are several important points need to be appropriately addressed before it can be accepted for publishing in Atmospheric Chemistry and Physics.*

We thank the referee for the careful reading and the valuable comments that helped improving our paper.

Detailed comments:

- 1. The impacts of biomass burning and topography on air quality in the North China Plain certainly are interesting topics for policy makers. However, because modeling results are sensitive from case to case, from policy perspectives, such kind of study should be conducted for a longer period. For the crop field burning, this paper only conducted a case study for one week in October. According to Figure 2 of this paper and other previous studies in China, the most intensive period of biomass burning in the eastern China is June. It's a little bit strange that the authors selected a case in October. In fact, from the results presented in Figure 5, it is quite clear that in this case the crop field burning activities didn't play an important role on air quality in both NNCP and SNCP if it was compared with an overall*

broad peak of anthropogenic pollution. For such kind of non-typical case, I don't know whether it is meaningful to make many statistics to compare the relative contributions in several tables (e.g. Tables 3-6). With such a short-term case, I would like suggest conducting more in-depth analysis to understand specific scientific questions other than a calculation of numbers.

We thank the referee for the thoughtful comment. This comment deals with several issues, and our responses are as follows:

- a. We selected a case study in October rather than in June, because the air pollution was extremely high (with maximum concentrations larger than $300 \mu\text{g}/\text{m}^3$) in NNCP, including Beijing, the capital city of China. It is important to understand the CFB contribution to the heavy air pollution in the incident.
- b. We agree with the referee that in order to get a solid conclusion from policy perspectives, multiply case studies are needed. We clarify that the purpose of this study is to get some insights of how could CFB affect the air quality in NNCP and Beijing under heavy haze condition. However, in order to get quantitative analysis, more and longer studies are needed.

Line 461-463, “We get some insights of how could CFB affect the air quality in NNCP and Beijing under heavy haze condition, though more and longer studies are needed to get more representative conclusions.”

- c. The selected study period is under a heavy aerosol pollution period. The relative daily average contributions reach to a maximum of 34% and 32% in SNCP and NNCP, respectively. However, by considering the heavy pollution ($> 300 \mu\text{g}/\text{m}^3$) in this period, a little over 30% is prominent.

Line 351-355, “Indeed, the CFB pollution plume go through a long-range transport to NNCP can cause an obvious increase to $\text{PM}_{2.5}$ concentration, with the maximum daily average contribution of 32% (Table 5). Such a high transported contribution indicates that the CFB is not only one of the significant local pollution sources, but also a considerable regional pollution source.”

- d. According to the referee's suggestions, we added more statistical results in Table 6, including the regional average changes in mass ($\mu\text{g}/\text{m}^3$) and percentage (%), and the lag-time of CFB pollution of NNCP from SNCP.

Line 370-388, “The pattern comparisons between simulated and observed near-surface $\text{PM}_{2.5}$ concentrations ($\text{TPM}_{2.5}$) perform well (Fig. 9 Left Panels). Meanwhile, the regional average CFB contributions are shown in Table 6, including mass concentration

and related percentage as well as the related lag-time of NNCP corresponding to SNCP. At T1, massive local pollutants are emitted from CFB in SNCP and the CFB plume had not yet been largely transported to NNCP (see **CPM_{2.5} of Fig. 9 T1**). The CFB contribution is high in SNCP with $72.6 \mu\text{g m}^{-3}$, accounting for 71% of the total PM_{2.5}, whereas the CFB contribution is low with $8.1 \mu\text{g m}^{-3}$ in NNCP, only accounting for 21%. At T2, high CFB contribution occurred in both SNCP and NNCP with $37 \mu\text{g m}^{-3}$, suggesting that plenty of CFB pollutants emitted from SNCP and had been transported to NNCP (see **CPM_{2.5} of Fig. 9 T2**). At T3, CFB contribution rapidly reduced in SNCP with $20.2 \mu\text{g m}^{-3}$ (13%). It is worth to note that the high CFB contribution with $50.4 \mu\text{g m}^{-3}$ (58%) is still remained in NNCP (see **CPM_{2.5} of Fig. 9 T3**). At T4, the CFB contribution largely decreased in both SNCP and NNCP (no more than 6%) (see **CPM_{2.5} of Fig. 9 T4**). The lag-time of NNCP to SNCP are 7-12 hours, and gradually increase from T1 to T4, implicating that the effect of CFB remains in longer time in NNCP than in SNCP. The highest PM_{2.5} concentrations are along the foothill of the Taihang Mountains (**Left panels of Fig. 9**), which may be related to the mountain effects.”

2. In the second part of this paper, the authors conducted an interesting numerical experiment by removing topography in specific regions in WRF-Chem model. However, such kind of treatment may cause some inconsistency in the initial conditions of meteorological parameters and the terrain data, which need more spin-up time because WRF uses a terrain-following vertical coordinate. However, according to the modeling description of this paper, the spin-up time for the WRF-Chem simulation is only 12 hours. Since the authors aim to give a quantitative understanding of the topographic effects, a longer spin-up time, for example several days, is needed. In addition, same as the Comment #1, as a case study for several days, the quantitative results here will have large uncertainty for policy makers. I would like suggest giving a more in-depth discussion by touching some scientific questions related to mountain, such as the impact of mountain-valley breezes on the accumulation of air pollutants etc.

- a. To address the comment of the referee, we extended the model spin-up time from 12 hours to 3 days (**Line 178**), and updated related results. We also added some shortcomings of the model study in the **Section 4.5 Impact of mountains**. As we stated in the above, we cannot give a quantitative analysis by the case study from policy perspectives, more cases and longer studies are needed.

Line 396-405, “In this study, we utilized the differences between the simulations with or without mountains to represent the effect of the topography on PM_{2.5} concentration, which were calculated based on Eq. (9). As an on-line dynamical model, the topography changes in WRF-CHEM can lead to dynamical changes, such as the wind speeds at the foothill of the mountains. This is a useful and traditional sensitivity analysis method for numerical model to quantify the mountains effects, but with some shortcomings, which are to bring uncertainties to the sensitivity experiment. Firstly, the impact of topography

is complicated to be completely quantified only by the altitude remove behavior. Secondly, the initial NCEP FNL data with mountains is treated as “real” in scenarios without mountains.”

- b. The guiding effect is treated as part of the mountain blocking effect. We modified and added the description in the revised paper.

Line 31-34, “...through the blocking effect. The mountains block and redirect the airflows, causing the pollutant accumulations along the foothill of mountains. This study suggests that the prohibition of CFB should be strict not just in or around Beijing, but also on the ulterior crop growth areas of SNCP.”

Line 418-423, “Here, it is attributed to the mountain blocking effect, which has two categories of influences. Firstly, the mountains block the airflows, causing pollutant accumulation and resulting in high $PM_{2.5}$ loading at the foothill of mountains (Influence-1, block). Secondly, the mountains redirect the airflows, causing the pollutants move toward the downwind foothill areas (Influence-2, redirect).”

Line 486-491, “Another major finding is that the mountains, surrounding the NCP in the north and west, play significant roles in enhancing the $PM_{2.5}$ pollution in NNCP through the blocking effect. Mountains block and redirect the airflows, causing the pollution accumulation along the foothill of mountains. The Taihang Mountains had greater impacts on $PM_{2.5}$ concentration than the Yanshan Mountains.”

Supplementary data of Fig. S3, “**Fig. S3** The schematic pictures of mountains effect along with the topography of the NCP region. (a) Mountains block the airflows and cause pollutants accumulated at the foothill of mountains. (b) Mountains redirect the airflows, and cause pollutants move toward the downwind foothill areas (Influence-2, redirect).”

3. The authors didn't give appropriate literature review for the both topics of biomass burning and topographic effect. In the model description part, the authors gave too many (more than 15) unnecessary references related to some common model schemes in WRF-Chem with some of them published several decades ago. However, in the main results part (Sect. 4), only two references (Cao et al., 2008 & Huang et al., 2012) are cited in the first paragraph but there is a lack of some comparisons of the results and conclusions with previous works done by other scientists for similar topics.

To address the comment of the referee, we added several revisions.

- a. A comprehensive summary of biomass burning emission topographic effect have been added in **Line 52-66** and **Line 80-91**, respectively.

Line 52-66, “However, CFB have adverse impacts on traffic conditions and ecology environments (Shi et al., 2014;Zhang, 2009), and release plenty of pollutants, such as CO, SO₂, VOC, NO_x and PM_{2.5} (Koppmann et al., 2005;Li et al., 2008). According to Guan et al. (2014) and Lu et al. (2011), annual CFB contribute about 13% of the total particulate matter (PM) emissions in China (Zhang et al., 2016). And it is more prominent during the harvest periods due to its strong seasonal dependence. Numerous studies have quantified the contribution of biomass burning and CFB to PM pollution in China. According to Yao et al. (2016), Cheng et al. (2013), Wang et al. (2009; 2007) and Song et al. (2007), biomass burning has important impacts on the ambient PM_{2.5} concentrations (15-24% in Beijing and 4-19% in Guangzhou). Yan et al. (2010) captured a heavy pollution with PM₁₀ concentrations higher than 350 $\mu\text{g m}^{-3}$ in some CFB locations. It is reported that CFB may contribute more than 30% of the PM₁₀ increase during CFB incidents (Zhu et al., 2012; Zha et al. 2013;Su et al., 2012). Cheng et al. (2014) report a summer case that CFB contributed 37% of PM_{2.5} concentrations in the Yangtze River delta.”

Line 80-91, “Yanshan and Taihang Mountains surround the NCP in the north and west (**Fig. 1c**). Such topography affects air pollution though PBL in complex ways (Miao et al., 2015b;Sun et al., 2013;Liu et al., 2009). Hu et al. (2014) have reported that the Loess Plateau and NCP result in a mountain-plains solenoid circulation, exacerbating air pollution over NCP. Chen et al. (2009) have founded that a mountain chimney effect is

dominated by mountain-valley breeze, enhancing the surface air pollution in Beijing. The mountain-plain breeze develops frequently in Beijing and may play important roles in modulating the local air quality (Miao et al., 2015b; Hu et al., 2014; Chen et al., 2009). Miao et al. (2015a) founded that the mountains played a significant role in the sea-land aerosol circulation and the pollutants could be transported and accumulated in the NCP areas along the mountains, which is treated as the blocking effect (Zhao et al., 2015).”

b. A more detailed model description was added in **Section 3.1 Model description**.

Line 153-160, “The specific version of WRF-CHEM model is developed by Li et al. (2010; 2011; 2012), with a new flexible gas phase chemical module and the CMAQ (version 4.6) aerosol module developed by US EPA (Binkowski and Roselle, 2003). The wet deposition follows the CMAQ method and the dry deposition is parameterized following Wesely (1989). The photolysis rates are calculated using the FTUV (Li et al., 2005; Tie et al., 2003), in which the impacts of aerosols and clouds on the photochemistry are considered (Li et al., 2011).”

Line 162-166, “Meanwhile, the ISORROPIA Version 1.7 (<http://nenes.eas.gatech.edu/ISORROPIA/>) is utilized to simulate the inorganic aerosols, which is primarily used to predict the thermodynamic equilibrium between the ammonia-sulfate-nitrate-chloride-water aerosols and their gas phase precursors of H_2SO_4 - HNO_3 - NH_3 - HCl -water vapor.”

Line 184-185, “The biogenic emissions are calculated on-line with the WRF-CHEM model using the MEGAN model (Guenther, 2006).”

c. We modified and added explicit statements of provincial CFB emission inventory processing in Line 192-197 and Line 210-221. And we updated the provincial statistical data and related results. The detailed results and related references were added in supplementary data of

Table S1, Table S2 and Table S3.

Line 192-197, “This situation may be resulted from the limitation of local enforcement of regulation despite CFB have already been banned (Zhang and Cao, 2015; Shi et al., 2014). The CFB have a seasonal pattern due to the post-harvest activities with two distinct peaks in summer and autumn, especially in June (33-59%) and October (6-19%) (**Fig. 2b**). The strong seasonal dependence character suggests that the CFB emissions during October are much larger than annual averages.”

Line 210-221, “where i stands for each province and k for different crop species of rice, corn and wheat. $E_{i,co}$ stands for CO emission from CFB of i -th province in gigagrams [Gg]. $P_{i,k}$ is the yield of crop in Gg. F_i is the proportion of residues burned in the field. D_k is the dry fraction of crop residue (dry matter). R_k is the residue-to-crop ratio (dry matter). CE_k is the combustion efficiency and EF_{co} is the emission factors of CFB. The $P_{i,k}$ values were taken from an official statistical yearbook (NBS, 2015) (**Table S1**), and the F_i on a provincial basis were taken from Wang and Zhang (2008) and Zhang Yisheng (Unpublished doctor thesis-in Chinese) (**Table S1**). The parameters of D_k , R_k , and CE_k are listed in **Table S2**. The EF_{co} from CFB was summarized range from 52 to 141 g kg⁻¹ in China (**Table S3**). In this study, we used 111 g kg⁻¹ as the average EF_{co} of crop residue, which was used to estimate the emissions from global open burning (Wiedinmyer et al., 2011).”

1 **Impact of crop field burning and mountains on heavy**
2 **haze in the North China Plain: A case study**

3 X. Long^{1,2}, X. X. Tie^{1,3,4,*}, J. J. Cao^{1,5}, R. J. Huang^{1,6,*}, T. Feng¹, N. Li^{1,7}, S. Y. Zhao¹,
4 J. Tian¹, G. H. Li¹, Q. Zhang⁸

5 (1) Key Lab of Aerosol Chemistry & Physics, SKLLQG, Institute of Earth Environment, Chinese
6 Academy of Sciences, Xi'an, 710061, China

7 (2) University of Chinese Academy of Sciences, Beijing, 100049, China

8 (3) [CAS Center for Excellence in Urban Atmospheric Environment \(CEUAE\), Xiamen, 361021, China](#)

9 (4) National Center for Atmospheric Research, Boulder, CO, 80303, USA

10 (5) Institute of Global Environmental Change, Xi'an Jiaotong University, Xi'an, 710049, China

11 (6) Laboratory of Atmospheric Chemistry, Paul Scherrer Institute (PSI), 5232 Villigen, Switzerland.

12 (7) Department of Atmospheric Science, National Taiwan University, Taipei, 10617, Taiwan

13 (8) Center for Earth System Science, Tsinghua University, Beijing, 100084, China

14 *Correspondence to:* X. X. Tie (xxtie@urcar.edu) R. J. Huang (rujin.huang@ieecas.cn)

Abstract. With the provincial statistical data and CFB activities captured by MODIS, we extracted a detailed CFB emission inventory in the North China Plain (NCP). The WRF-CHEM model is applied to investigate the impact of CFB on air pollution during the period from October 6 to 12, 2014, corresponding to a heavy haze incident with high concentrations of PM_{2.5} (particulate matter with aerodynamic diameter less than 2.5 μm). The WRF-CHEM model generally performs well in simulating the surface species concentrations of PM_{2.5}, O₃ and NO₂ compared to the observations. And reasonably reproduced the observed temporal variations of wind speed, wind direction and planetary boundary layer height (PBLH). It is found that the CFB occurred in southern NCP (SNCP) have significant effects on PM_{2.5} concentrations locally, causing a maximum of 34% PM_{2.5} increase. Under the continuously southerly wind condition, the CFB pollution plume go through a long-range transport to northern NCP (NNCP-with several mega cities, including Beijing, the capital city of China), where few CFB occurred, resulting in a maximum of 32% PM_{2.5} increase. As a result, the heavy haze in Beijing is enhanced by the CFB occurred in SNCP. Mountains also play significant roles in enhancing the PM_{2.5} pollution in NNCP through the blocking effect. The mountains block and redirect the airflows, causing the pollutant accumulations along the foothill of mountains. This study suggests that the prohibition of CFB should be strict not just in or around Beijing, but also on the ulterior crop growth areas of SNCP. PM_{2.5} emissions in SNCP should be significantly limited in order to reduce the occurrences of heavy haze events in NNCP region.

Key words: crop field burning; mountain effect; PM_{2.5}; WRF-CHEM

1 Introduction

Crop residue burning is important for global biomass burning (Yevich and Logan, 2003;Shon, 2015), especially in agricultural countries such as China. Crop residue resources in China rank the first in the world, accounting for 17.3% of the global production (Bi et al., 2010), and increasing with the average annual proportion of 4% (Hong et al., 2015;Zhao et al., 2010). Compared with other approaches, crop field burning (CFB) is the most effective and less expensive to remove residues. The national annual average proportion of CFB to total residues is about 11-25%(Cao et al., 2008;Hao and Liu, 1994;Streets et al., 2003;Wang and Zhang, 2008;Zhao et al., 2010). Large numbers of annual CFB occur in China (Zhang et al., 2015; Yan et al., 2006), especially during the post-harvest seasons (Zhang et al., 2016;Shi et al., 2014;Cao et al., 2008). And most of the CFB occur on crop growth areas, such as the North China Plain (NCP) (Huang et al., 2012;Li et al., 2008), where have been frequently suffering haze events in recent years (Yang et al., 2015;Jiang et al., 2015;Wang et al., 2013;Wang et al., 2012).

However, CFB have adverse impacts on traffic conditions and ecology environments (Shi et al., 2014;Zhang, 2009), and release plenty of pollutants, such as CO, SO₂, VOC, NO_x and PM_{2.5} (Koppmann et al., 2005;Li et al., 2008). According to Guan et al. (2014) and Lu et al. (2011), annual CFB contribute about 13% of the total particulate matter (PM) emissions in China (Zhang et al., 2016). And it is more prominent during the harvest periods due to its strong seasonal dependence. Numerous studies have quantified the contribution of biomass burning and CFB to

PM pollution in China. According to Yao et al. (2016), Cheng et al. (2013), Wang et al. (2009; 2007) and Song et al. (2007), biomass burning has important impacts on the ambient PM_{2.5} concentrations (15-24% in Beijing and 4-19% in Guangzhou). Yan et al. (2010) captured a heavy pollution with PM₁₀ concentrations higher than 350 µg m⁻³ in some CFB locations. It is reported that CFB may contribute more than 30% of the PM₁₀ increase during CFB incidents (Zhu et al., 2012; Zha et al. 2013; Su et al., 2012). Cheng et al. (2014) report a summer case that CFB contributed 37% of PM_{2.5} concentrations in the Yangtze River delta.

The impact of CFB to air quality is continental and regional. Air quality in China is influenced by the CFB occurred in Southeast Asia and on the Indian Peninsula (Qin et al., 2006). Mukai et al. (2014) have reported that CFB emissions in Southeast Asia contribute the carbonaceous aerosols in Beijing. Within China, the inter-province transported air pollutants emitted from CFB significantly affect regional PM levels and air quality (Cheng et al., 2014; Zhu et al., 2012). For Beijing, the smoke particles from CFB are expected to be one of the major components (Wang et al., 2014; Cheng et al., 2013), though the percentage of transported sources are seldom specified (Zhang et al., 2016). A recent study reports that CFB and regional transport illustrate two of the key processes of haze formation in October 2014, especially on Oct. 6th, but without quantitative estimation in this work (Yang et al., 2015). Related quantification studies are of great importance for the control strategies of CFB in Beijing.

Yanshan and Taihang Mountains surround the NCP in the north and west (**Fig. 1c**). Such topography affects air pollution through PBL in complex ways (Miao et al., 2015b; Sun et al., 2013; Liu et al., 2009). Hu et al. (2014) have reported that the Loess Plateau and NCP result in a mountain-plains solenoid circulation, exacerbating air pollution over NCP. Chen et al. (2009) have founded that a mountain chimney effect is dominated by mountain-valley breeze, enhancing the surface air pollution in Beijing. The mountain-plain breeze develops frequently in Beijing and may play important roles in modulating the local air quality (Miao et al., 2015b; Hu et al., 2014; Chen et al., 2009). Miao et al. (2015a) founded that the mountains played a significant role in the sea-land aerosol circulation and the pollutants could be transported and accumulated in the NCP areas along the mountains, which is treated as the blocking effect (Zhao et al., 2015).

In this study, we analyzed a heavy haze episode occurred in NCP region from "LT" 12:00 6th to 00:00 12th October in 2014. During the period, the average PM_{2.5} concentrations are much higher than class II standard in both SNCP and NNCP. The characteristics of the air pollution were analyzed based on PM_{2.5} concentration. Depending on the satellite-based observations of Moderate Resolution Imaging Spectroradiometer (MODIS), a large number of CFB occurred in SNCP, whereas few CFB happened in NNCP. A more detailed CFB emission inventory was extracted. Thereafter we analyzed the regional transport of CFB emissions from SNCP to NNCP driven by prevailing southerly winds. Under the continuously southerly wind condition, the mountains play important roles for the northward transport, and cause

the accumulation of the aerosol pollutants at the foothill of the mountains. We also analyzed the impact of mountains (especially the Taihang Mountains and the Yanshan Mountains) on the air pollution transport.

2 Description of data

2.1 Geographical Location

In order to study the effect of CFB on local and regional air pollution, the research domain locates in eastern China, covering a large regional area (more than 10 provinces) (see **Fig. 1a**). The NCP region is in the middle of the research domain, with two mountains in the north and west. The Yanshan Mountains locate in the north of NCP with east-west directions, and the Taihang Mountains locate in the west of NCP with southwest-northeast directions (**Fig. 1b**). **Figure 1c** displays the distribution of online sampling sites and CFB captured by MODIS during the haze episodes. We defined two regions of interests according to CFB occurrences, topographic conditions, industrial and agricultural developments. One is the northern NCP (NNCP), including two mega cities (Beijing and Tianjin) and the north part of Hebei province, where only few CFB occurred. Another is the southern NCP (SNCP), where substantial CFB occurred during the haze episodes as shown in **Fig. 1c**. Because of the severe haze problem in the capital city of China (Beijing), one of the main focuses is to study the long-range transport of CFB pollution from SNCP to NNCP.

2.2 Meteorological conditions

The reanalysis meteorological data, including wind direction, wind speed and PBLH were obtained from the European Centre for Medium-range Weather Forecasts (ECMWF), with a spatial resolution of $0.125^{\circ} \times 0.125^{\circ}$. The data is available at: <http://www.ecmwf.int/products/data/>. The average wind direction and wind speed are displayed in **Table 1**. During the haze episode, the mean wind directions are 174.8° in NNCP and 165.2° in SNCP, and the average wind speeds are 2.4 m s^{-1} in both NNCP and SNCP. The results suggest that the prevailing winds are continuously southerly winds with weak wind speeds, which is favorable to the pollution long-range transport from SNCP to NNCP, which has been reported as one of the major contributors to haze formation in the Beijing City (Tie et al., 2015).

2.3 PM_{2.5} Measurements

The hourly PM_{2.5} mass concentration were continuously monitored by the Ministry of Environmental Protection (MEP) of China (<http://datacenter.mep.gov.cn>), including 5 sites in NNCP and 7 sites in SNCP (indicated by green crosses in **Fig. 1c**). The data was updated from the website: <http://www.pm25.in/>. **Table 1** summarizes the site information and the observed PM_{2.5} concentrations. During the study period, the average PM_{2.5} concentrations are $200.0 \mu\text{g m}^{-3}$ in NNCP and $184.1 \mu\text{g m}^{-3}$ in SNCP. The measured PM_{2.5} concentrations are much higher than class II standard (daily mean of $75 \mu\text{g m}^{-3}$), indicating an occurrence of heavy pollution event. We analyzed the characteristics of the air pollution based on PM_{2.5} concentration simulated by

WRF-CHEM. Meanwhile, it is worth to note that the highest PM_{2.5} concentrations occurred along the foothill sites of the Taihang Mountains. At the foothill sites of BJ, BD, SJZ and XT, PM_{2.5} concentrations are 245.5, 287.7, 257.9, and 320.1 $\mu\text{g m}^{-3}$, respectively. The mean PM_{2.5} concentration in these 4 sites is 277.8 $\mu\text{g m}^{-3}$, much higher than 147.2 $\mu\text{g m}^{-3}$ averaged from the other sites. Considering the continuously southerly winds and the topographic conditions, we studied the impact of the mountains on the air pollution transport.

3 Methods

3.1 Model description

We use Weather Research and Forecasting Chemical model (WRF-CHEM) (Grell et al., 2005) to simulate the spatial and temporal variability of PM_{2.5} concentration. The specific version of WRF-CHEM model is developed by Li et al. (2010; 2011; 2012), with a new flexible gas phase chemical module and the CMAQ (version 4.6) aerosol module developed by US EPA (Binkowski and Roselle, 2003). The wet deposition follows the CMAQ method and the dry deposition is parameterized following Wesely (1989). The photolysis rates are calculated using the FTUV (Li et al., 2005; Tie et al., 2003), in which the impacts of aerosols and clouds on the photochemistry are considered (Li et al., 2011). The gas-phase chemistry was represented in the model by the modified RADM2 (Regional Acid Deposition Model, version 2) gas-phase chemical mechanism (Stockwell et al., 1990; Chang et al., 1987). Meanwhile, the ISORROPIA Version 1.7 (<http://nenes.eas.gatech.edu/ISORROPIA/>) is utilized to

simulate the inorganic aerosols, which is primarily used to predict the thermodynamic equilibrium between the ammonia-sulfate-nitrate-chloride-water aerosols and their gas phase precursors of H_2SO_4 - HNO_3 - NH_3 - HCl -water vapor. The Yonsei University (YSU) PBL scheme (Hong et al., 2006), Lin microphysics scheme (Lin et al., 1983), Noah land-surface model (Chen and Dudhia, 2001) were utilized. The model has been successfully applied in several regional pollution studies (Tie et al., 2009; Tie et al., 2007; He et al., 2015).

The WRF-CHEM model is configured with resolution of 6×6 km (200×300 grid cells) centered in (117°E , 39°N). Vertical layers extend from the surface to 50 hPa, with 28 vertical layers, involving 7 layers in the bottom of 1 km. The meteorological initial and boundary conditions were gathered from NCEP FNL Operational Global Analysis data. The lateral chemical initial conditions were constrained by a global chemical transport model-MOZART4 (Model for Ozone and Related chemical Tracers, Version 4) 6-hour output (Emmons et al., 2010; Tie et al., 2005). For the episode simulations, the spin-up time of the WRF-CHEM model is 3 days.

The surface emission inventory used in this study was obtained from the Multi-resolution Emission Inventory for China (MEIC) (Zhang et al., 2009), which is an update and improvement for the year 2010 (<http://www.meicmodel.org>). The emission inventory estimated only anthropogenic emission such as non-residential sources (transportation, agriculture, industry and power) and residential sources related to fuel combustions. The biogenic emissions are calculated on-line with the WRF-CHEM model using the MEGAN model (Guenther, 2006). Additionally, we

added emission from CFB in the present study.

3.2 Crop field burning emissions

We analyzed the annual and monthly number of open crop fire events captured by MODIS in the research domain from 2008 to 2014. In the NCP region, the CFB activities gradually increase from the minimum fire events of 12, 000 times in 2008 to 27, 000 times in 2014 (Fig. 2a), suggesting that the CFB is not efficiently controlled in this region. This situation may be resulted from the limitation of local enforcement of regulation despite CFB have already been banned (Zhang and Cao, 2015;Shi et al., 2014). The CFB have a seasonal pattern due to the post-harvest activities with two distinct peaks in summer and autumn, especially in June (33-59%) and October (6-19%) (Fig. 2b). The strong seasonal dependence character suggests that the CFB emissions during October are much larger than annual averages. In order to have the detailed horizontal distribution of the pollutant emissions of CFB, we elaborated a method to generate emission inventory using the satellite data of “MODIS Thermal Anomalies/Fire product (MOD/MYD14DL)”. The MOD/MYD14DL product can detect small opening fires ($<100\text{ m}^2$) (Giglio et al., 2003) and produce the geographic location of open fire activities (van der Werf et al., 2006). In this study, the CFB was defined as MOD/MYD14DL active fires occurred over the cropland, which is classified by the MODIS Combined Land Cover Type product (Friedl et al., 2010). Firstly, we estimated the CO emission of CFB, utilizing a widely used method (Streets et al., 2003;Cao et al., 2008;Zhang et al., 2008;Ni et al., 2015a) based on the

annual provincial statistical data. The provincial emission of crop residues burning can be calculated by Eq. (1):

$$E_{i,CO} = \sum_{k=1}^3 P_{i,k} \times F_i \times D_k \times R_k \times CE_k \times EF_{co} \quad (1)$$

where i stands for each province and k for different crop species of rice, corn and wheat. $E_{i,co}$ stands for CO emission from CFB of i -th province in gigagrams [Gg]. $P_{i,k}$ is the yield of crop in Gg. F_i is the proportion of residues burned in the field. D_k is the dry fraction of crop residue (dry matter). R_k is the residue-to-crop ratio (dry matter). CE_k is the combustion efficiency and EF_{co} is the emission factors of CFB. The $P_{i,k}$ values were taken from an official statistical yearbook (NBS, 2015) (**Table S1**), and the F_i on a provincial basis were taken from Wang and Zhang (2008) and Zhang Yisheng (Unpublished doctor thesis-in Chinese) (**Table S1**). The parameters of D_k , R_k , and CE_k are listed in **Table S2**. The EF_{co} from CFB was summarized range from 52 to 141 g kg⁻¹ in China (**Table S3**). In this study, we used 111 g kg⁻¹ as the average EF_{co} of crop residue, which was used to estimate the emissions from global open burning (Wiedinmyer et al., 2011).

The provincial CO emission was temporally and spatially allocated according to the CFB activities. The detailed daily CO emission of k -th grid ($E_{k,co}$) was calculated using Eq. (2):

$$E_{k,CO} = \frac{FC_k}{FC_i} \times E_{i,CO} , \quad (2)$$

where FC_k and FC_i are the total CFB fire counts in k -th grid and i -th province, respectively (**Table S1**).

Thereafter, the emissions of various gaseous and particulate species (E_{spec1}) were calculated by the Eq. (3). And individual chemical compounds (E_{spec2}) were calculated by Eq. (4).

$$E_{k,spec1} = \frac{EF_{spec1}}{EF_{CO}} \times E_{k,CO}, \quad (3)$$

$$E_{k,spec2} = E_{k,NMOC} \times scale, \quad (4)$$

where $E_{k,spec1}$ and $E_{k,spec2}$ are the k -th grid emission of the specify WRF-CHEM species; E_{spec1} and EF_{CO} are the emission factors of CFB; $E_{k,NMOC}$ is NMOC emission in the k -th grid calculated by Eq. (3); $scale$ is the value to convert NMOC emissions to WRF-CHEM chemical species. The emission factors for gaseous and particulate species and $scale$ to convert NMOC emissions to WRF-CHEM chemical species from CFB were taken from available datasets (Wiedinmyer et al., 2011; Akagi et al., 2011; Andreae and Merlet, 2001), which were summarized by Wiedinmyer et al. (2011) (Table 2).

4 Results and discussions

4.1 Evaluate the Crop field burning emission

The provincial CO emissions of CFB were estimated based on Eq. (1), and there was 8.2 Tg CO emitted from CFB in 2014 (Table S1). This result is comparable to previous studies, which is 4.6-10.1 Tg yr⁻¹ (Cao et al., 2008; Ni et al., 2015; Streets et al., 2003; Yan et al., 2006). According to the MODIS observations, a large number of CFB occurred in SNCP, including provinces of Henan with 61% and Shandong with 22%. Most of CFB occurred on Oct. 6th and 7th, accounting for 75% (Table 3).

Table 4 shows the CFB emissions of gaseous and particulate species on Oct. 6th and 7th, including the mega cities of Beijing and Tianjin, and provinces of Hebei, Henan and Shandong in NCP. **Figure 3** displays the CFB activities and related CO emission on Oct. 6th and 7th. Most of the pollutants are emitted from Henan in SNCP, accounting for 73% on Oct. 6th and 65% on Oct. 7th. Plenty of pollutants emitted from CFB on Oct. 6th, producing more than 5.1 Gg PM_{2.5} and 98.0 Gg CO (1 Gg = 10⁹ g).

4.2 Statistical characteristics of the evaluation

The characteristics of the haze pollution were defined by PM_{2.5} concentration, which is significantly affected by the local wind fields and PBLH in the NCP region (Tie et al., 2015). In order to evaluate the model performance, the model simulations were compared with the measured results in both species concentrations (PM_{2.5}, O₃ and NO₂) and meteorological parameters (wind speed, wind direction and PBLH). The normalized mean bias (NMB) and correlation coefficient (R) were used to quantify the performance.

$$NMB = \frac{\sum_{i=1}^N (P_i - O_i)}{\sum_{i=1}^N O_i}, \quad (5)$$

$$R = \frac{\sum_{i=1}^N (P_i - \bar{P})(O_i - \bar{O})}{[\sum_{i=1}^N (P_i - \bar{P})^2 \sum_{i=1}^N (O_i - \bar{O})^2]^{\frac{1}{2}}}, \quad (6)$$

where P_i is the predicted results and O_i represents the related observations. N is the total number of the predictions used for comparisons. Meanwhile, \bar{P} and \bar{O} are the average prediction and related mean observation, respectively.

Figure 4 shows the measured and calculated temporal variations of regional average species concentrations, including PM_{2.5}, O₃ and NO₂. The WRF-CHEM model

reproduced the pollution episode well, with a good agreement with observations. The correlation coefficients (R) of simulated and measured PM_{2.5} concentrations are 0.88 in both NNCP and SNCP (**Fig. 4a**). The simulations are overall lower than the observations with NMB of -12% in NNCP and -7% in SNCP. Considering the high average PM_{2.5} concentration with 200.0 $\mu\text{g m}^{-3}$ in NNCP and 184.1 $\mu\text{g m}^{-3}$ in SNCP, obvious underestimates exist with the overall concentrations of 24.0 $\mu\text{g m}^{-3}$ in NNCP and 12.9 $\mu\text{g m}^{-3}$ in SNCP. This may be related to the CMAQ (version 4.6) aerosol module, which is likely to underestimated OM due to the uncertainty in secondary organic aerosols mechanism (Baek et al., 2011). Meanwhile, the underestimates are also related to the negative bias in S3, which may be related to cloud contamination (**Fig. S1**). Whereas this has only a few impacts on the estimation of CFB contribution since few CFB occurred during S3. The simulations of O₃ and NO₂ are also agree well with observations, with R greater than 0.77 and absolute NMB lower than 17% (**Fig. 4b and 4c**). **Figure 5** displays the measured and calculated temporal variations of regional average meteorological parameters, including wind speed, wind direction, and the PBLH in both NNCP and SNCP. The comparisons between simulated and observed wind fields show good agreements (**Fig. 5a and 5b**), with all the R higher than 0.64, and the absolute NMB are no more than 15%. Meanwhile, the R of PBLH is larger than 0.88 and the absolute NMB is no more than 10% (**Fig. 5c**).

4.3 Characteristics of the heavy pollution events

According to the evolution of PM_{2.5} concentration (**Fig. 4a**), the haze episode can be

divided into three stages: (I) pollution formation stage (S1, 12:00 6th - 00:00 8th), (II) pollution outbreak stage (S2, 00:00 8th - 00:00 10th) and (III) pollution clear stage (S3, 00:00 10th - 00:00 12th). The major characteristics of each stage are briefly summarized below. Related simulations in bracket follow the detailed observations.

- S1 (pollution formation): It is dominated by a continuously southerly wind, with mean wind speed of 2.5 (2.7) m s⁻¹ in NNCP and 3.0 (3.6) m s⁻¹ in SNCP. The backward trajectories, with the HYSPLIT model online version, of BJ, TJ and BD during S1 reflected how the CFB influenced the NNCP region (Fig. 6). The air mass mainly came from the south, originating from the SNCP region. The pollutants are continuously transported from SNCP to NNCP, leading to pollutants accumulation in NNCP, which is characterized by the steady rising of PM_{2.5} concentration in NNCP from 20.6 (41.0) µg m⁻³ (at 12:00 Oct. 6th) to 242.7 (217.5) µg m⁻³ (at 00:00 Oct. 8th) (Fig. 4 a1).

- S2 (pollution outbreak): During S2, the air pollution deteriorates. It is a relative stable period of heavy pollution with average PM_{2.5} concentration of 252.0 (241.2) µg m⁻³ in NNCP and 214.1 (235.0) µg m⁻³ in SNCP, which are higher than those in other stages. This phenomenon may be related to the relative lower wind speed and PBLH.

- S3 (pollution clear): During S3, the southerly winds gradually decrease, and turn to be northerly at the end of S3. Clean airs from the north region of China obviously improve the air quality. Compared with S2, the average PM_{2.5} concentrations are decreased in both NNCP and SNCP.

There were several important issues shown in the results, and should be addressed. (1) The $PM_{2.5}$ concentrations are extremely high during the S2 period, and the daily average concentrations are greater than the Chinese National Standard ($75 \mu g m^{-3}$) by 2-3 times. (2) The air pollutions are severe in a large region (occurred in both NNCP and SNCP). (3) During the S1 and S2 periods, there is a time lag between SNCP and NNCP for $PM_{2.5}$ concentrations. Because it is a continuously southerly wind condition, it shows the important impact of long-range transport of $PM_{2.5}$ particles from the SNCP to NNCP.

4.4 Contributions of crop field burning

Model sensitivity studies were conducted to separate the individual CFB contribution. Two model simulations were performed, i.e., one with both anthropogenic and CFB emissions while the other with only anthropogenic emission. We calculated $PM_{2.5}$ distributions by including CFB emissions (anthropogenic and CFB) and excluding CFB emissions (only anthropogenic). In this study, the CFB contributions were quantified by regional average contribution in mass concentration ($CPM_{2.5}$) and daily average contribution proportion ($\overline{PPM}_{2.5}$).

$$CPM_{2.5} = TPM_{2.5} - APM_{2.5}, \quad (7)$$

$$\overline{PPM}_{2.5} = \frac{\overline{CPM}_{2.5}}{\overline{TPM}_{2.5}}, \quad (8)$$

where $TPM_{2.5}$ represents the simulated $PM_{2.5}$ concentrations considering total emission; $APM_{2.5}$ denotes the simulated $PM_{2.5}$ concentrations only considering anthropogenic emissions. $\overline{CPM}_{2.5}$ and $\overline{TPM}_{2.5}$ are daily average value for $CPM_{2.5}$

and $TPM_{2.5}$, respectively.

Figure 7 displays the regional observed and simulated $PM_{2.5}$ concentrations considering total emissions (anthropologic and CFB) and only anthropologic emissions. It is clearly shown that the CFB had important contributions to $PM_{2.5}$ in both NNCP (**Fig. 7a**) and SNCP **Fig. 7b**). This is also proved by the daily average contribution proportion ($\overline{PPM}_{2.5}$) of CFB (**Table 5**). The high values of $\overline{PPM}_{2.5}$ in SNCP appear on Oct 6th with 34% and on 7th with 17%, when plenty of CFB occurred. Simultaneously, the high values of $\overline{PPM}_{2.5}$ in NNCP appear on Oct 7th with 32% and 8th with 10%, showing a later occurrence than that in SNCP. The time lag suggests that the plume with CFB may be transported from SNCP to NNCP.

The detailed hourly CFB contributions to $PM_{2.5}$ concentrations ($CPM_{2.5}$) are displayed in **Fig. 8**. The values of $CPM_{2.5}$ in NNCP are generally lag synchronized with that in SNCP, such as P_{N1} versus P_{S1} and P_{N2} versus P_{S2} (**Fig. 8a and 8b**). Apparently, the lagged time is not constant and varied with the wind fields. The specific details perform relaxed lag synchronized, especially between the P_{N2} and P_{S2} . This phenomenon further indicates that the CFB contribution in SNCP is mainly due to local emission, whereas CFB contribution in NNCP is largely resulted from long-range transport from SNCP. Indeed, the CFB pollution plume go through a long-range transport to NNCP can cause an obvious increase to $PM_{2.5}$ concentration, with the maximum daily average contribution of 32% (**Table 5**). Such a high transported contribution indicates that the CFB is not only one of the significant local pollution sources, but also a considerable regional pollution source.

356 To clearly show the time evolution of the CFB effect on $PM_{2.5}$ concentration, four
 357 time-points were defined in **Fig. 8c**, such as T1 (23:00 6th), T2 (05:00 7th), T3 (20:00
 358 7th) and T4 (19:00 8th). At T1, prominent CFB contribution occurred in SNCP with
 359 the highest value of $71.9 \mu g m^{-3}$, but accompanied with unimportant CFB contribution
 360 in NNCP with a low value of $7.7 \mu g m^{-3}$. At T2, the CFB contribution in SNCP
 361 decline with a relative high value of $44.2 \mu g m^{-3}$, but rise in NNCP with $51.6 \mu g m^{-3}$
 362 (near the transition between P1 and P2). At T3, the CFB contribution rapidly
 363 decreases to a low value of $24.0 \mu g m^{-3}$ in SNCP, but increase to the highest with 47.0
 364 $\mu g m^{-3}$ in NNCP. At T4, the CFB contributions largely decrease, becoming lesser in
 365 both SCNP ($9.1 \mu g m^{-3}$) and NNCP ($11.4 \mu g m^{-3}$). Interestingly, the CFB contribution
 366 in SNCP drops faster than that in NNCP (**P2 in Fig. 8c**), resulting in stronger effects
 367 in NNCP than in SNCP, as well as longer effects in NNCP.

368 To further understand the evolution of CFB to heavy haze pollution, we analyzed the
 369 horizontal distributions of $PM_{2.5}$ concentration ($TPM_{2.5}$) and related CFB contribution
 370 ($CPM_{2.5}$) at T1, T2, T3 and T4 (**Fig. 9**). The pattern comparisons between simulated
 371 and observed near-surface $PM_{2.5}$ concentrations ($TPM_{2.5}$) perform well (**Fig. 9 Left**
 372 **Panels**). Meanwhile, the regional average CFB contributions are shown in **Table 6**,
 373 including mass concentration and related percentage as well as the related lag-time of
 374 NNCP corresponding to SNCP. At T1, massive local pollutants are emitted from CFB
 375 in SNCP and the CFB plume had not yet been largely transported to NNCP (see
 376 $CPM_{2.5}$ of **Fig. 9 T1**). The CFB contribution is high in SNCP with $72.6 \mu g m^{-3}$,
 377 accounting for 71% of the total $PM_{2.5}$, whereas the CFB contribution is low with 8.1

$\mu\text{g m}^{-3}$ in NNCP, only accounting for 21%. At T2, high CFB contribution occurred in both SNCP and NNCP with $37 \mu\text{g m}^{-3}$, suggesting that plenty of CFB pollutants emitted from SNCP and had been transported to NNCP (see *CPM_{2.5}* of Fig. 9 T2). At T3, CFB contribution rapidly reduced in SNCP with $20.2 \mu\text{g m}^{-3}$ (13%). It is worth to note that the high CFB contribution with $50.4 \mu\text{g m}^{-3}$ (58%) is still remained in NNCP (see *CPM_{2.5}* of Fig. 9 T3). At T4, the CFB contribution largely decreased in both SNCP and NNCP (no more than 6%) (see *CPM_{2.5}* of Fig. 9 T4). The lag-time of NNCP to SNCP are 7-12 hours, and gradually increase from T1 to T4, implicating that the effect of CFB remains in longer time in NNCP than in SNCP. The highest $\text{PM}_{2.5}$ concentrations are along the foothill of the Taihang Mountains (Left panels of Fig. 9), which may be related to the mountain effects.

4.5 Impact of mountains

Sensitivity experiments were conducted to quantify the impacts of the Taihang Mountains (referred as R-T), the Yanshan Mountains (R-Y) and both of them (R-TY) on the heavy pollution. The mountains were removed from the model calculation, in which, the altitude of mountains were reduced to the average altitude of NCP (30 m). With the reduction of altitudes of the topography, the dynamical conditions calculated from WRF-CHEM changed, which affect pollutions transport, especially along the foothill of mountains. In this study, we utilized the differences between the simulations with or without mountains to represent the effect of the topography on $\text{PM}_{2.5}$ concentration, which were calculated based on Eq. (9). As an on-line dynamical

model, the topography changes in WRF-CHEM can lead to dynamical changes, such as the wind speeds at the foothill of the mountains. This is a useful and traditional sensitivity analysis method for numerical model to quantify the mountains effects, but with some shortcomings, which are to bring uncertainties to the sensitivity experiment. Firstly, the impact of topography is complicated to be completely quantified only by the altitude remove behavior. Secondly, the initial NCEP FNL data with mountains is treated as “real” in scenarios without mountains. The sensitive configuration and related enclosing scope are displayed in **Fig. S2**.

$$IPM_{2.5} = RPM_{2.5} - TPM_{2.5}, \quad (9)$$

where $IPM_{2.5}$ is the net impacts of mountains on $PM_{2.5}$; $RPM_{2.5}$ denotes the simulated $PM_{2.5}$ concentration with removal behaviors, involving R-TY, R-T, and R-Y; $TPM_{2.5}$ represents the simulated $PM_{2.5}$ concentration considering emission of anthropologic and CFB, which is correspond with the case of R0 (**Fig. S2a**).

The sensitivity study period was selected from 12:00 7th to 00:00 10th. **Fig. 10** displays the elevation contours and the horizontal distributions of $PM_{2.5}$ concentration with the effect of mountains, exhibiting a good performance of the pattern comparisons between simulated and observed near-surface $PM_{2.5}$ concentrations. The results illustrate that the mountains had important impacts on regional $PM_{2.5}$ concentration, especially for the region along the foothill of mountains with a heavy pollution area, covering sampling sites of BJ, BD, SJZ and XT. Here, it is attributed to the mountain blocking effect, which has two categories of influences. Firstly, the mountains block the airflows, causing pollutant accumulation and resulting in high

PM_{2.5} loading at the foothill of mountains (Influence-1, block). Secondly, the mountains redirect the airflows, causing the pollutants move toward the downwind foothill areas (Influence-2, redirect). Both influences act to prevent the pollutant plume to disperse toward western mountains, causing accumulations of the air pollutants along the foothill of mountains. These two influences of mountain blocking effect are illustrated as the schematic pictures in **Fig. S3**.

Fig. 11 displays the simulated PM_{2.5} concentration due to the mountain effects (*RPM_{2.5}*), with the three cases (R-TY, R-T, and R-Y). The heavy pollution accumulation (**Fig. 10**) along the foothill of mountains is significantly reduced, especially with the removal of Taihang Mountains (R-T, and R-TY) (**Fig. 11 a1 and a2**). In these two cases, the pollution plumes dispersed westerly (**Fig. 11 b1 and b2**). The PM_{2.5} concentrations increase 40-120 $\mu\text{g m}^{-3}$ in the western part of Taihang Mountains, and reduce 20-60 $\mu\text{g m}^{-3}$ in NCP. The distribution of the reduced pollution plume shows a northeast band plume, *indicating the mountain blocking effect*. With the removal of the Yanshan Mountains (R-Y), the high PM_{2.5} concentrations are still remained along the foothill of the Taihang Mountains (**Fig. 11 a3**), but more pollutants are pushed forward along the foothill, toward the northeastern NCP. Without the blocking effect of the Yanshan Mountains, the PM_{2.5} concentrations increased 20-80 $\mu\text{g m}^{-3}$ in the northern part of the Yanshan Mountains, and decreased 10-60 $\mu\text{g m}^{-3}$ in the southern part of the Yanshan Mountains (**Fig. 11 b3**).

In the foothill sampling sites (BJ, BD, SJZ and XT), the average PM_{2.5} concentrations are reduced 54.2 $\mu\text{g m}^{-3}$ for the case of R-T, which is much higher than the case of

R-Y ($28.4 \mu\text{g m}^{-3}$). For the other non-foothill sites, the average reduction is $34.7 \mu\text{g m}^{-3}$ for the case of R-T, which is also much higher than the case of R-Y ($2.4 \mu\text{g m}^{-3}$), suggesting that the Taihang Mountains have stronger effects than the Yanshan Mountains. Meanwhile, the higher impacts in the foothill sampling sites than non-foothill sites are further demonstrated.

5 Conclusions

In recent years, the NCP region, including the capital city of Beijing, has been suffering serious haze pollution problem, especially in winter and summer. Most studies concerned about the intense secondary formation, huge regional transport of pollutants, stationary meteorological conditions and large local emission. In autumn, CFB and movement of wind based on large scale topography are important in NCP, whereas the percentage of transported CFB emission sources are seldom specified. This is probably resulted from the contingency of CFB activities during harvest period and the limitation of temporal resolution of CFB emission inventories. In this study, we extracted a more detailed CFB emission inventory based on the provincial statistical data and CFB activities captured by MODIS. The WRF-CHEM mode was applied to study the effect of CFB on the $\text{PM}_{2.5}$ concentrations in NCP, especially the evaluation of CFB plums pollution, such as local influence and long-range transportation. We get some insights of how could CFB affect the air quality in NNCP and Beijing under heavy haze condition, though more and longer studies are needed to get more representative conclusions. The results are summarized:

- (1) A more detailed CFB emission inventory was generated in NCP. The daily CFB emissions were estimated depending on CFB activities captured by MODIS. Plenty of pollutants emitted from SNCP on Oct. 6th and 7th, producing plenty of PM_{2.5} pollution, but few in NNCP during the entire haze period.
- (2) The WRF-CHEM model reproduced the pollution episode with a good agreement with observations. The correlation coefficients (R) of simulated and measured PM_{2.5} concentration are 0.88 in both NNCP and SNCP, and the related NMB are -12% in NNCP and -7% in SNCP. The simulated winds and PBLH are also in good agreement with observations in both NNCP and SNCP.
- (3) The WRF-CHEM model was used to investigate the impacts of CFB contribution and its evaluation on PM_{2.5} concentration. The SNCP region is mainly influenced by the local CFB emissions, causing a maximum of 34% PM_{2.5} increase. Whereas the NNCP region is mainly affected by the long-range transport of pollution plume emitted from CFB in SNCP, causing a maximum of 32% PM_{2.5} increase in NNCP.
- (4) The research domain includes two regions of interests. One is the NNCP, including two mega cities (Beijing and Tianjin), where few CFB occurred. Another is the SNCP, where substantial CFB occurred. This study shows that there are substantially long-transport of CFB plume from SNCP to NNCP. More importantly, the effect of CFB remains in longer time in NNCP than in SNCP along the foothill areas of the Taihang Mountains, causing significant enhancement in Beijing in both time and magnitude.

(5) Another major finding is that the mountains, surrounding the NCP in the north and west, play significant roles in enhancing the $PM_{2.5}$ pollution in NNCP through the blocking effect. Mountains block and redirect the airflows, causing the pollution accumulation along the foothill of mountains. The Taihang Mountains had greater impacts on $PM_{2.5}$ concentration than the Yanshan Mountains.

On account of various factors, such as pollutant long-range transport and pollutant accumulation caused by mountain effects, the prohibition of CFB should be strict not just in or around Beijing, but also on the ulterior crop growth areas of SNCP. Other $PM_{2.5}$ emissions in the SNCP should be significantly limited in order to reduce the occurrences of heavy haze events in NNCP region, including the Beijing City.

Acknowledgement

The PBL height and wind field data was obtained from the European Centre for Medium-Range Weather Forecasts (ECMWF) website (<http://www.ecmwf.int/products/data/>). This work is supported by the National Natural Science Foundation of China (NSFC) under Grant Nos. 41275186 and 41430424, and the Open Fund of the State Key Laboratory of Loess and Quaternary Geology (SKLLQG1413). The National Center for Atmospheric Research is sponsored by the National Science Foundation.

506 **Reference**

- 507 Akagi, S., Yokelson, R. J., Wiedinmyer, C., Alvarado, M., Reid, J., Karl, T., Crounse, J.,
508 and Wennberg, P.: Emission factors for open and domestic biomass burning for use
509 in atmospheric models, *Atmospheric Chemistry and Physics*, 11, 4039-4072, 2011.
- 510 Andreae, M. O., and Merlet, P.: Emission of trace gases and aerosols from biomass
511 burning, *Global biogeochemical cycles*, 15, 955-966, 2001.
- 512 Baek, J., Hu, Y., Odman, M. T., and Russell, A. G.: Modeling secondary organic
513 aerosol in CMAQ using multigenerational oxidation of semi-volatile organic
514 compounds, *Journal of Geophysical Research: Atmospheres*, 116, 2011.
- 515 Bi, Y., Wang, Y., and Cao, C.: Straw Resource Quantity and its Regional Distribution in
516 China [J], *Journal of Agricultural Mechanization Research*, 3, 1-7, 2010.
- 517 Binkowski, F. S., and Roselle, S. J.: Models-3 Community Multiscale Air Quality
518 (CMAQ) model aerosol component 1. Model description, *Journal of Geophysical*
519 *Research: Atmospheres*, 108, 2003.
- 520 Cao, G., Zhang, X., Wang, Y., and Zheng, F.: Estimation of emissions from field
521 burning of crop straw in China, *Chinese Science Bulletin*, 53, 784-790, 2008.
- 522 Chang, J., Brost, R., Isaksen, I., Madronich, S., Middleton, P., Stockwell, W., and
523 Walcek, C.: A three-dimensional Eulerian acid deposition model: Physical concepts
524 and formulation, *Journal of Geophysical Research: Atmospheres* (1984–2012), 92,
525 14681-14700, 1987.
- 526 Chen, F., and Dudhia, J.: Coupling an advanced land surface-hydrology model with the
527 Penn State-NCAR MM5 modeling system. Part I: Model implementation and
528 sensitivity, *Monthly Weather Review*, 129, 569-585, 2001.
- 529 Chen, Y., Zhao, C., Zhang, Q., Deng, Z., Huang, M., and Ma, X.: Aircraft study of
530 mountain chimney effect of Beijing, china, *Journal of Geophysical Research:*
531 *Atmospheres*, 114, 2009.
- 532 Cheng, Y., Engling, G., He, K.-B., Duan, F.-K., Ma, Y.-L., Du, Z.-Y., Liu, J.-M., Zheng,

533 M., and Weber, R. J.: Biomass burning contribution to Beijing aerosol, *Atmospheric*
 534 *Chemistry and Physics*, 13, 7765-7781, 2013.

535 Cheng, Z., Wang, S., Fu, X., Watson, J., Jiang, J., Fu, Q., Chen, C., Xu, B., Yu, J., and
 536 Chow, J.: Impact of biomass burning on haze pollution in the Yangtze River delta,
 537 China: a case study in summer 2011, *Atmospheric Chemistry and Physics*, 14,
 538 4573-4585, 2014.

539 Dudhia, J.: Numerical study of convection observed during the winter monsoon
 540 experiment using a mesoscale two-dimensional model, *Journal of the Atmospheric*
 541 *Sciences*, 46, 3077-3107, 1989.

542 Emmons, L., Walters, S., Hess, P., Lamarque, J.-F., Pfister, G., Fillmore, D., Granier, C.,
 543 Guenther, A., Kinnison, D., and Laepple, T.: Description and evaluation of the
 544 Model for Ozone and Related chemical Tracers, version 4 (MOZART-4),
 545 *Geoscientific Model Development*, 3, 43-67, 2010.

546 Friedl, M. A., Sulla-Menashe, D., Tan, B., Schneider, A., Ramankutty, N., Sibley, A.,
 547 and Huang, X.: MODIS Collection 5 global land cover: Algorithm refinements and
 548 characterization of new datasets, *Remote Sensing of Environment*, 114, 168-182,
 549 2010.

550 Giglio, L., Descloitres, J., Justice, C. O., and Kaufman, Y. J.: An enhanced contextual
 551 fire detection algorithm for MODIS, *Remote sensing of environment*, 87, 273-282,
 552 2003.

553 Grell, G. A., Peckham, S. E., Schmitz, R., McKeen, S. A., Frost, G., Skamarock, W. C.,
 554 and Eder, B.: Fully coupled “online” chemistry within the WRF model,
 555 *Atmospheric Environment*, 39, 6957-6975, 2005.

556 Guan, D., Su, X., Zhang, Q., Peters, G. P., Liu, Z., Lei, Y., and He, K.: The
 557 socioeconomic drivers of China’s primary PM_{2.5} emissions, *Environmental*
 558 *Research Letters*, 9, 024010, 2014.

559 Guenther, C.: Estimates of global terrestrial isoprene emissions using MEGAN (Model
 560 of Emissions of Gases and Aerosols from Nature), *Atmospheric Chemistry and*
 561 *Physics*, 6, 2006.

562 Hao, W.-M., and Liu, M.-H.: Spatial and temporal distribution of tropical biomass
563 burning, *Global biogeochemical cycles*, 8, 495-503, 1994.

564 He, H., Tie, X., Zhang, Q., Liu, X., Gao, Q., Li, X., and Gao, Y.: Analysis of the causes
565 of heavy aerosol pollution in Beijing, China: A case study with the WRF-CHEM
566 model, *Particuology*, 20, 32-40, 2015.

567 Hong, J., Ren, L., Hong, J., and Xu, C.: Environmental impact assessment of corn straw
568 utilization in China, *Journal of Cleaner Production*, 30, 1e9, 2015.

569 Hong, S.-Y., Noh, Y., and Dudhia, J.: A new vertical diffusion package with an explicit
570 treatment of entrainment processes, *Monthly Weather Review*, 134, 2318-2341,
571 2006.

572 Hu, X.-M., Ma, Z., Lin, W., Zhang, H., Hu, J., Wang, Y., Xu, X., Fuentes, J. D., and
573 Xue, M.: Impact of the Loess Plateau on the atmospheric boundary layer structure
574 and air quality in the North China Plain: A case study, *Science of The Total
575 Environment*, 499, 228-237, 2014.

576 Huang, X., Li, M., Li, J., and Song, Y.: A high-resolution emission inventory of crop
577 burning in fields in China based on MODIS Thermal Anomalies/Fire products,
578 *Atmospheric Environment*, 50, 9-15, 2012.

579 Jiang, C., Wang, H., Zhao, T., Li, T., and Che, H.: Modeling study of PM 2.5 pollutant
580 transport across cities in China's Jing-Jin-Ji region during a severe haze episode in
581 December 2013, *Atmospheric Chemistry and Physics*, 15, 5803-5814, 2015.

582 Koppmann, R., Czapiewski, K. v., and Reid, J.: A review of biomass burning emissions,
583 part I: gaseous emissions of carbon monoxide, methane, volatile organic compounds,
584 and nitrogen containing compounds, *Atmospheric Chemistry and Physics
585 Discussions*, 5, 10455-10516, 2005.

586 Li, G., Zhang, R., Fan, J., and Tie, X.: Impacts of black carbon aerosol on photolysis
587 and ozone, *Journal of Geophysical Research: Atmospheres*, 110, 2005.

588 Li, G., Lei, W., Zavala, M., Volkamer, R., Dusanter, S., Stevens, P., and Molina, L.:
589 Impacts of HONO sources on the photochemistry in Mexico City during the

590 MCMA-2006/MILAGO Campaign, *Atmospheric Chemistry and Physics*, 10,
591 6551-6567, 2010.

592 Li, G., Bei, N., Tie, X., and Molina, L.: Aerosol effects on the photochemistry in
593 Mexico City during MCMA-2006/MILAGRO campaign, *Atmospheric Chemistry*
594 *and Physics*, 11, 5169-5182, 2011.

595 Li, G., Lei, W., Bei, N., and Molina, L.: Contribution of garbage burning to chloride and
596 PM 2.5 in Mexico City, *Atmospheric Chemistry and Physics*, 12, 8751-8761, 2012.

597 Li, L., Wang, Y., Zhang, Q., Li, J., Yang, X., and Jin, J.: Wheat straw burning and its
598 associated impacts on Beijing air quality, *Science in China Series D: Earth Sciences*,
599 51, 403-414, 2008.

600 Lin, Y.-L., Farley, R. D., and Orville, H. D.: Bulk parameterization of the snow field in
601 a cloud model, *Journal of Climate and Applied Meteorology*, 22, 1065-1092, 1983.

602 Liu, S., Liu, Z., Li, J., Wang, Y., Ma, Y., Sheng, L., Liu, H., Liang, F., Xin, G., and
603 Wang, J.: Numerical simulation for the coupling effect of local atmospheric
604 circulations over the area of Beijing, Tianjin and Hebei Province, *Science in China*
605 *Series D: Earth Sciences*, 52, 382-392, 2009.

606 Lu, Z., Zhang, Q., and Streets, D. G.: Sulfur dioxide and primary carbonaceous aerosol
607 emissions in China and India, 1996–2010, *Atmospheric Chemistry and Physics*, 11,
608 9839-9864, 2011.

609 Miao, Y., Liu, S., Zheng, Y., and Wang, S.: Modeling the feedback between aerosol and
610 boundary layer processes: a case study in Beijing, China, *Environmental Science*
611 *and Pollution Research*, 1-16, 2015a.

612 Miao, Y., Liu, S., Zheng, Y., Wang, S., and Chen, B.: Numerical study of the effects of
613 topography and urbanization on the local atmospheric circulations over the
614 Beijing-Tianjin-Hebei, China, *Advances in Meteorology*, 2015, 2015b.

615 Mlawer, E. J., Taubman, S. J., Brown, P. D., Iacono, M. J., and Clough, S. A.: Radiative
616 transfer for inhomogeneous atmospheres: RRTM, a validated correlated-k model for
617 the longwave (Paper 97JD00237), *JOURNAL OF GEOPHYSICAL*

618 RESEARCH-ALL SERIES-, 102, 16,663-616,682, 1997.

619 Mukai, S., Yasumoto, M., and Nakata, M.: Estimation of biomass burning influence on
620 air pollution around Beijing from an aerosol retrieval model, *The Scientific World*
621 *Journal*, 2014, 2014.

622 National Bureau of Statistics (NBS), 2015. *China Statistical Yearbook 2014*. China
623 Statistics Press, Beijing. <http://www.stats.gov.cn/tjsj/ndsj/2015/indexch.htm>.

624 Ni, H., Han, Y., Cao, J., Chen, L.-W. A., Tian, J., Wang, X., Chow, J. C., Watson, J. G.,
625 Wang, Q., and Wang, P.: Emission characteristics of carbonaceous particles and
626 trace gases from open burning of crop residues in China, *Atmospheric Environment*,
627 123, 399-406, 2015.

628 Qin, S.-g., Ding, A., and Wang, T.: Transport pattern of biomass burnings air masses in
629 Eurasia and the impacts on China, *China Environmental Science*, 26, 641-645, 2006.

630 Shi, T., Liu, Y., Zhang, L., Hao, L., and Gao, Z.: Burning in agricultural landscapes: an
631 emerging natural and human issue in China, *Landscape Ecology*, 29, 1785-1798,
632 2014.

633 Shon, Z.-H.: Long-term variations in PM 2.5 emission from open biomass burning in
634 Northeast Asia derived from satellite-derived data for 2000–2013, *Atmospheric*
635 *Environment*, 107, 342-350, 2015.

636 Song, Y., Tang, X., Xie, S., Zhang, Y., Wei, Y., Zhang, M., Zeng, L., and Lu, S.:
637 Source apportionment of PM2. 5 in Beijing in 2004, *Journal of Hazardous Materials*,
638 146, 124-130, 2007.

639 Stockwell, W. R., Middleton, P., Chang, J. S., and Tang, X.: The second generation
640 regional acid deposition model chemical mechanism for regional air quality
641 modeling, *Journal of Geophysical Research: Atmospheres* (1984–2012), 95,
642 16343-16367, 1990.

643 Streets, D., Yarber, K., Woo, J. H., and Carmichael, G.: Biomass burning in Asia:
644 Annual and seasonal estimates and atmospheric emissions, *Global Biogeochemical*
645 *Cycles*, 17, 2003.

646 Su, J., Zhu, B., Kang, H., Wang, H., and Wang, T.: Applications of pollutants released
 647 form crop residues at open burning in Yangtze River Delta region in air quality
 648 model, *Environmental Science*, 33, 1418-1424, 2012.

649 Sun, Y., Song, T., Tang, G., and Wang, Y.: The vertical distribution of PM 2.5 and
 650 boundary-layer structure during summer haze in Beijing, *Atmospheric Environment*,
 651 74, 413-421, 2013.

652 Tie, X., Madronich, S., Walters, S., Zhang, R., Rasch, P., and Collins, W.: Effect of
 653 clouds on photolysis and oxidants in the troposphere, *Journal of Geophysical*
 654 *Research: Atmospheres*, 108, 2003.

655 Tie, X., Madronich, S., Walters, S., Edwards, D. P., Ginoux, P., Mahowald, N., Zhang,
 656 R., Lou, C., and Brasseur, G.: Assessment of the global impact of aerosols on
 657 tropospheric oxidants, *Journal of Geophysical Research: Atmospheres* (1984–2012),
 658 110, 2005.

659 Tie, X., Madronich, S., Li, G., Ying, Z., Zhang, R., Garcia, A. R., Lee-Taylor, J., and
 660 Liu, Y.: Characterizations of chemical oxidants in Mexico City: A regional chemical
 661 dynamical model (WRF-CHEM) study, *Atmospheric Environment*, 41, 1989-2008,
 662 2007.

663 Tie, X., Geng, F., Peng, L., Gao, W., and Zhao, C.: Measurement and modeling of O₃
 664 variability in Shanghai, China: Application of the WRF-CHEM model, *Atmospheric*
 665 *Environment*, 43, 4289-4302, 2009.

666 Tie, X., Zhang, Q., He, H., Cao, J., Han, S., Gao, Y., Li, X., and Jia, X. C.: A budget
 667 analysis of the formation of haze in Beijing, *Atmospheric Environment*, 100, 25-36,
 668 2015.

669 van der Werf, G. R., Randerson, J. T., Giglio, L., Collatz, G. J., Kasibhatla, P. S., and
 670 Arellano Jr, A. F.: Interannual variability in global biomass burning emissions from
 671 1997 to 2004, *Atmospheric Chemistry and Physics*, 6, 3423-3441, 2006.

672 Wang, L., Xu, J., Yang, J., Zhao, X., Wei, W., Cheng, D., Pan, X., and Su, J.:
 673 Understanding haze pollution over the southern Hebei area of China using the
 674 CMAQ model, *Atmospheric Environment*, 56, 69-79, 2012.

675 Wang, L., Wei, Z., Yang, J., Zhang, Y., Zhang, F., Su, J., Meng, C., and Zhang, Q.: The
676 2013 severe haze over southern Hebei, China: model evaluation, source
677 apportionment, and policy implications, *Atmos. Chem. Phys*, 14, 3151-3173, 2013.

678 Wang, Q., Shao, M., Liu, Y., William, K., Paul, G., Li, X., Liu, Y., and Lu, S.: Impact
679 of biomass burning on urban air quality estimated by organic tracers: Guangzhou
680 and Beijing as cases, *Atmospheric Environment*, 41, 8380-8390, 2007.

681 Wang, Q., Shao, M., Zhang, Y., Wei, Y., Hu, M., and Guo, S.: Source apportionment of
682 fine organic aerosols in Beijing, *Atmospheric Chemistry and Physics*, 9, 8573-8585,
683 2009.

684 Wang, S., and Zhang, C.: Spatial and temporal distribution of air pollutant emissions
685 from open burning of crop residues in China, *Sciencepaper online*, 3, 329-333,
686 2008.

687 Wang, W., Maenhaut, W., Yang, W., Liu, X., Bai, Z., Zhang, T., Claeys, M., Cachier,
688 H., Dong, S., and Wang, Y.: One-year aerosol characterization study for PM 2.5
689 and PM 10 in Beijing, *Atmospheric Pollution Research*, 5, 554-562, 2014.

690 Wesely, M.: Parameterization of surface resistances to gaseous dry deposition in
691 regional-scale numerical models, *Atmospheric Environment* (1967), 23, 1293-1304,
692 1989.

693 Wiedinmyer, C., Akagi, S., Yokelson, R. J., Emmons, L., Al-Saadi, J., Orlando, J., and
694 Soja, A.: The Fire INventory from NCAR (FINN): A high resolution global model
695 to estimate the emissions from open burning, *Geoscientific Model Development*, 4,
696 625, 2011.

697 Yan, X., Ohara, T., and Akimoto, H.: Bottom-up estimate of biomass burning in
698 mainland China, *Atmospheric Environment*, 40, 5262-5273, 2006.

699 Yang, Y., Liu, X., Qu, Y., An, J., Jiang, R., Zhang, Y., Sun, Y., Wu, Z., Zhang, F., and
700 Xu, W.: Characteristics and formation mechanism of continuous hazes in China: a
701 case study during the autumn of 2014 in the North China Plain, *Atmospheric*
702 *Chemistry and Physics*, 15, 8165-8178, 2015.

703 Yao, L., Yang, L., Yuan, Q., Yan, C., Dong, C., Meng, C., Sui, X., Yang, F., Lu, Y.,
 704 and Wang, W.: Sources apportionment of PM 2.5 in a background site in the North
 705 China Plain, *Science of The Total Environment*, 541, 590-598, 2016.

706 Yevich, R., and Logan, J. A.: An assessment of biofuel use and burning of agricultural
 707 waste in the developing world, *Global biogeochemical cycles*, 17, 2003.

708 Zha, S., Zhang, S., Cheng, T., Chen, J., Huang, G., Li, X., and Wang, Q.: Agricultural
 709 fires and their potential impacts on regional air quality over China, *Aerosol Air Qual*
 710 *Res*, 13, 992-1001, 2013.

711 Zhang, H.: A laboratory study on emission characteristics of gaseous and particulate
 712 pollutants emitted from agricultural crop residue burning in China, Ph. D Thesis,
 713 Fudan University, China, 2009.

714 Zhang, L., Liu, Y., and Hao, L.: Contributions of open crop straw burning emissions to
 715 PM2. 5 concentrations in China, *Environmental Research Letters*, 11, 014014, 2016.

716 Zhang, Q., Streets, D. G., Carmichael, G. R., He, K. B., Huo, H., Kannari, A., Klimont,
 717 Z., Park, I. S., Reddy, S., Fu, J. S., Chen, D., Duan, L., Lei, Y., Wang, L. T., and
 718 Yao, Z. L.: Asian emissions in 2006 for the NASA INTEx-B mission, *Atmospheric*
 719 *Chemistry and Physics*, 9, 5131-5153, 2009.

720 Zhang, Y.-L., and Cao, F.: Is it time to tackle PM 2.5 air pollutions in China from
 721 biomass-burning emissions?, *Environmental Pollution*, 202, 217-219, 2015.

722 Zhang, Z., Gao, J., Engling, G., Tao, J., Chai, F., Zhang, L., Zhang, R., Sang, X., Chan,
 723 C.-y., and Lin, Z.: Characteristics and applications of size-segregated biomass
 724 burning tracers in China's Pearl River Delta region, *Atmospheric Environment*, 102,
 725 290-301, 2015.

726 Zhao, L., Leng, Y., Ren, H., and Li, H.: Life cycle assessment for large-scale
 727 centralized straw gas supply project, *Journal of Anhui Agri Sci*, 38, 19462-19464,
 728 2010.

729 Zhao, S., Tie, X., Cao, J., and Zhang, Q.: Impacts of mountains on black carbon aerosol
 730 under different synoptic meteorology conditions in the Guanzhong region, China,

731 Atmospheric Research, 164, 286-296, 2015.

732 Zhu, J., Wang, T., Deng, J., Jiang, A., and Liu, D.: An emission inventory of air

733 pollutants from crop residue burning in Yangtze River Delta Region and its

734 application in simulation of a heavy haze weather process, Acta Scientiae

735 Circumstantiae, 32, 3045-3055, 2012.

736

737

738

Figure Captions

739 Figure 1 The study area, sampling sites and crop fires. (a) The research domain and
740 related provinces in China. (b) Topographical conditions of North China
741 Plain. (c) Location of sampling sites and crop field burning captured by
742 MODIS during the haze episodes. Green crosses indicate the measurement
743 sites, and the CFB are shown by the pink dots.

744 Figure 2 The (a) yearly and (b) monthly crop field burning observed by MODIS in the
745 research domain during the year of 2008 to 2014.

746 Figure 3 Crop field burning captured by MODIS with the background of MODIS
747 real-time true color map (Left) and related CO emission (Right) on Oct. 6th
748 and 7th.

749 Figure 4 Regional averaged temporal variations in simulated (in red) and observed (in
750 blue) results of species concentrations of (a) PM_{2.5} (b) O₃ and (c) NO₂ over
751 the regions of NNCP and SNCP.

752 Figure 5 Regional averaged temporal variations in simulated (in red) and observed (in
753 blue) results of meteorological parameters of (a) wind speed (b) wind
754 direction and (c) PBLH over the regions of NNCP and SNCP.

755 Figure 6 Backward trajectories of NNCP (Beijing, Tianjin and Baoding) during S1
756 (LST, 12:00 6th - 00:00 8th) in different height of 100m, 500m and 1000m.

757 Figure 7 Hourly PM_{2.5} concentration of observations (obs) and simulations (sim-total
758 and sim-anthro) in (a) NNCP and (b) SNCP. Sim-total represents the
759 simulations considering total emissions (anthropologic and crop field
760 burning), whereas sim-anthro is the simulations only considering
761 anthropologic emissions.

762 Figure 8 CFB contribution to PM_{2.5} concentration ($CPM_{2.5}$) (a) in SNCP, (b) in NNCP
763 and (c) their comparison. The key point-in-local-times of T1 (23:00 6th), T2
764 (05:00 7th), T3 (20:00 7th) and T4 (19:00 8th) are signed with blue arrow.

Figure 9 The distributions of $TPM_{2.5}$ and $CPM_{2.5}$ of the key point-in-local-times of T1, T2, T3 and T4, which represent different pollution phase of emission from crop field burning to $PM_{2.5}$. Left panels also show the pattern comparisons of simulated vs. observed near-surface $PM_{2.5}$ concentrations ($TPM_{2.5}$), with $PM_{2.5}$ observations of colored circles. Black arrows denote simulated surface winds.

Figure 10 The elevation contours and the pattern comparisons of simulated vs. observed near-surface $PM_{2.5}$ concentrations from 12:00 7th to 00:00 10th. Colored circles: $PM_{2.5}$ observations of foothill sites; Colored squares: $PM_{2.5}$ observations of non-foothill sites; Black arrows: simulated surface winds. The 200-meter contour was highlighted with bold black line.

Figure 11 The averaged spatial distribution of $PM_{2.5}$ concentration and horizontal winds during 12:00 7th to 00:00 10th. (a) Simulated $PM_{2.5}$ loading with erase behavior $RPM_{2.5}$, involving R-TY, R-T, and R-Y. (b) The related impacts of mountains to $PM_{2.5}$ ($IPM_{2.5}$), which represents the net effect of related mountains. The bold black lines were used to stress enclosing scope of each erased behavior.

Table 1. The average PM_{2.5} concentration, wind direction and wind speed of the observations from 12:00 6th to 00:00 12th. The sampling sites located at the foot of mountains were emphasized with bold style.

Region	Site	Longitude (°E)	Latitude (°N)	PM _{2.5} (μg/m ³)	Wind-dir (°)	Wind-sp (m/s)
	Beijing (BJ)	116.41	40.04	245.5	185.8	2.2
	Langfang (LF)	116.73	39.56	214.7	177.0	2.4
	Tianjin (TJ)	117.31	39.09	134.7	173.5	2.4
	Baoding (BD)	115.49	38.87	287.7	171.2	2.2
	Cangzhou (CZ)	116.87	38.31	117.3	166.6	2.5
	NNCP			200.0	174.8	2.35
	Shijiazhuang (SJZ)	114.49	38.04	257.9	175.2	2.0
	Hengshui (HS)	115.68	37.74	166.7	163.7	2.6
	Dezhou (DZ)	116.31	37.47	152.4	162.7	2.6
	Xingtai (XT)	114.50	37.09	320.1	198.1	2.3
	Liaocheng (LC)	116.00	36.46	139.7	158.4	2.6
	Hezhe (HZ)	115.46	35.26	105.0	138.9	2.4
	Zhengzhou (ZZ)	113.66	34.79	146.9	159.2	2.4
	SNCP			184.1	165.2	2.42

Table 2. The gaseous and particulate species emission factors (g/kg) and scales to convert NMOC emissions (kg day^{-1}) to WRF/Chem chemical species (moles-species day^{-1}) from crop field burning. The detailed chemical species are described by Stockwell et al. (1990).

Gaseous species							Particulate species					
CO ¹	NOx ¹	NO ¹	NO ₂ ²	SO ₂ ³	NH3 ¹	NMOC ¹	OC ³	BC ³	PM _{2.5} ¹			
111	3.5	1.7	3.9	0.4	2.3	57	3.3	0.69	5.8			
Chemical-compounds-to-NMOC scales ^{1,2}												
ETH	HC3	HC5	OL2	OLT	OLI	TOL	CSL	HCHO	ALD	KET	ORA2	ISO
0.43	0.73	0.07	1.09	0.27	0.20	1.07	0.49	1.84	3.05	0.83	2.19	0.60

a. The values were taken from Andreae and Merlet (2001); b. The values were taken from Wiedinmyer et al., (2011); c. The values were taken from Akagi et al., (2011)

Table 3. The fire counts of crop field burning detected by the MODIS in the provinces over NCP during the haze episode (from Oct. 6th to 11th, 2014).

Province	6-Oct	7-Oct	8-Oct	9-Oct	10-Oct	11-Oct	Percentage
Beijing	0	0	0	0	0	0	0%
Tianjin	0	0	0	0	0	0	0%
Hebei	60	11	14	1	5	6	10%
Henan	370	104	59	18	19	23	61%
Shandong	100	54	9	9	32	7	22%
Anhui	6	6	20	0	10	3	5%
Shanxi	3	0	0	3	4	1	1%
Jiangsu	4	3	5	0	3	1	2%
Percentage	56%	18%	11%	3%	8%	4%	100%

Table 4. The emissions (Gg/day) of gaseous and particulate species from crop field burning on Oct. 6th and Oct. 7th in NCP region, including the provinces of Beijing, Tianjin, Hebei, Henan, Shandong.

Time	Province	CO	NO _x	NO	NO ₂	NMOC	SO ₂	NH ₃	PM _{2.5}	OC	BC
6-Oct	Beijing	0.00	0.00	0.00	0.00	0.00	0.00	0.00	0.00	0.00	0.00
	Tianjin	0.00	0.00	0.00	0.00	0.00	0.00	0.00	0.00	0.00	0.00
	Hebei	10.58	0.33	0.16	0.37	5.44	0.04	0.22	0.55	0.31	0.07
	Henan	71.17	2.24	1.09	2.50	36.55	0.26	1.47	3.72	2.12	0.44
	Shandong	16.27	0.51	0.25	0.57	8.35	0.06	0.34	0.85	0.48	0.10
	Total	98.0	3.1	1.5	3.4	50.3	0.4	2.0	5.1	2.9	0.6
7-Oct	Beijing	0.00	0.00	0.00	0.00	0.00	0.00	0.00	0.00	0.00	0.00
	Tianjin	0.00	0.00	0.00	0.00	0.00	0.00	0.00	0.00	0.00	0.00
	Hebei	1.94	0.06	0.03	0.07	1.00	0.01	0.04	0.10	0.06	0.01
	Henan	20.01	0.63	0.31	0.70	10.27	0.07	0.41	1.05	0.59	0.12
	Shandong	8.79	0.28	0.13	0.31	4.51	0.03	0.18	0.46	0.26	0.05
	Total	30.7	1.0	0.5	1.1	15.8	0.1	0.6	1.6	0.9	0.2

807 Table 5. Average contribution proportion of crop field burning to PM_{2.5} concentration.

808

Region	6-Oct.	7-Oct.	8-Oct.	9-Oct.	10-Oct.	11-Oct.
NNCP	5%	32%	10%	3%	2%	4%
SNCP	34%	17%	6%	3%	1%	1%

809

810

Table 6. The regional average contribution of CFB in mass concentration and percentage, and the lag-time of NNCP to SNCP for the four time-points of T1 (23:00 6th), T2 (05:00 7th), T3 (20:00 7th) and T4 (19:00 8th).

Time	Mass ($\mu\text{g}/\text{m}^3$)		Percentage		Lag-time (hours)
	NNCP	SNCP	NNCP	SNCP	
T1	8.1	72.6	21%	71%	7
T2	36.7	36.5	73%	27%	8
T3	50.4	20.2	58%	13%	11
T4	13.4	10.3	6%	5%	12

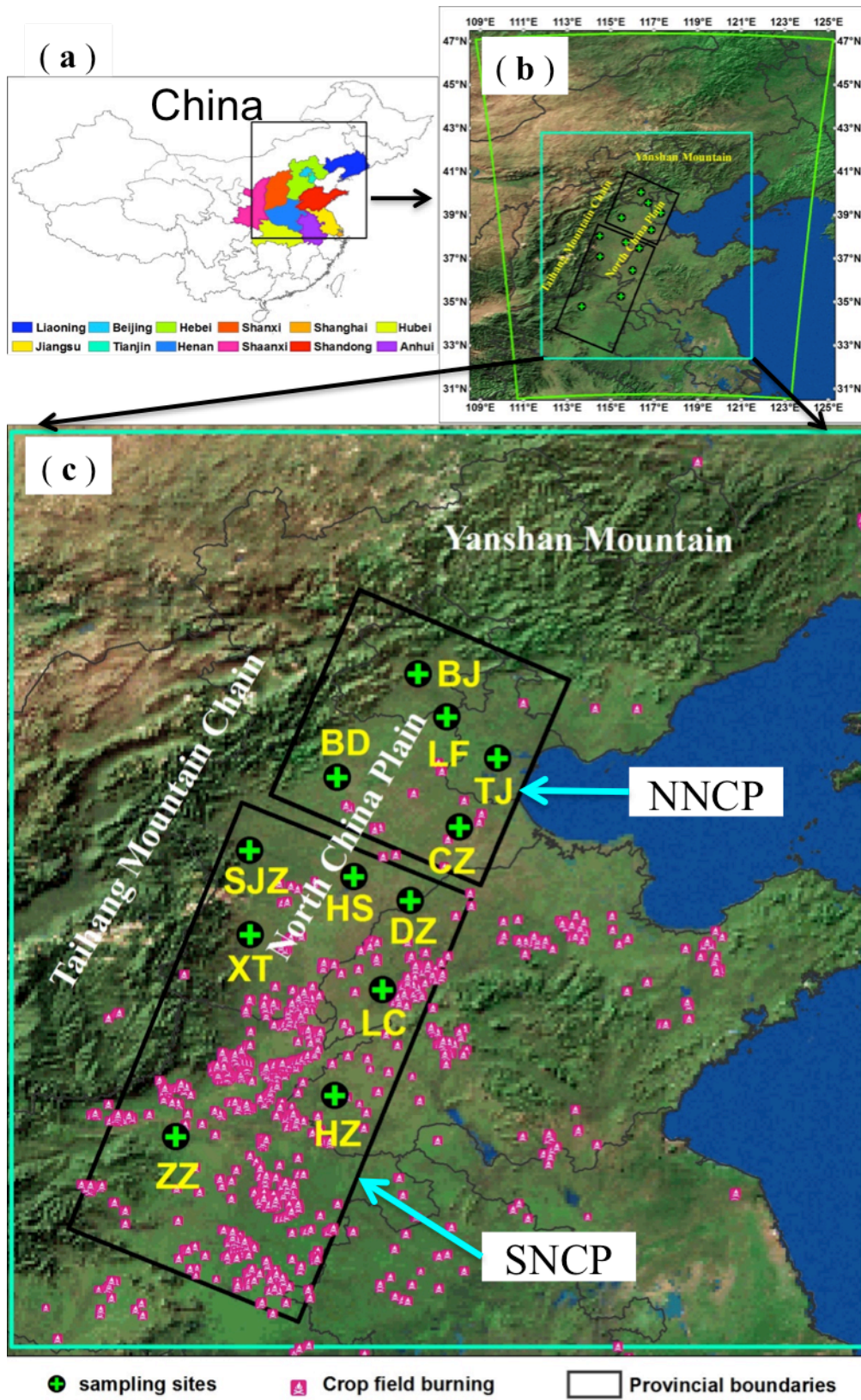


Figure 1

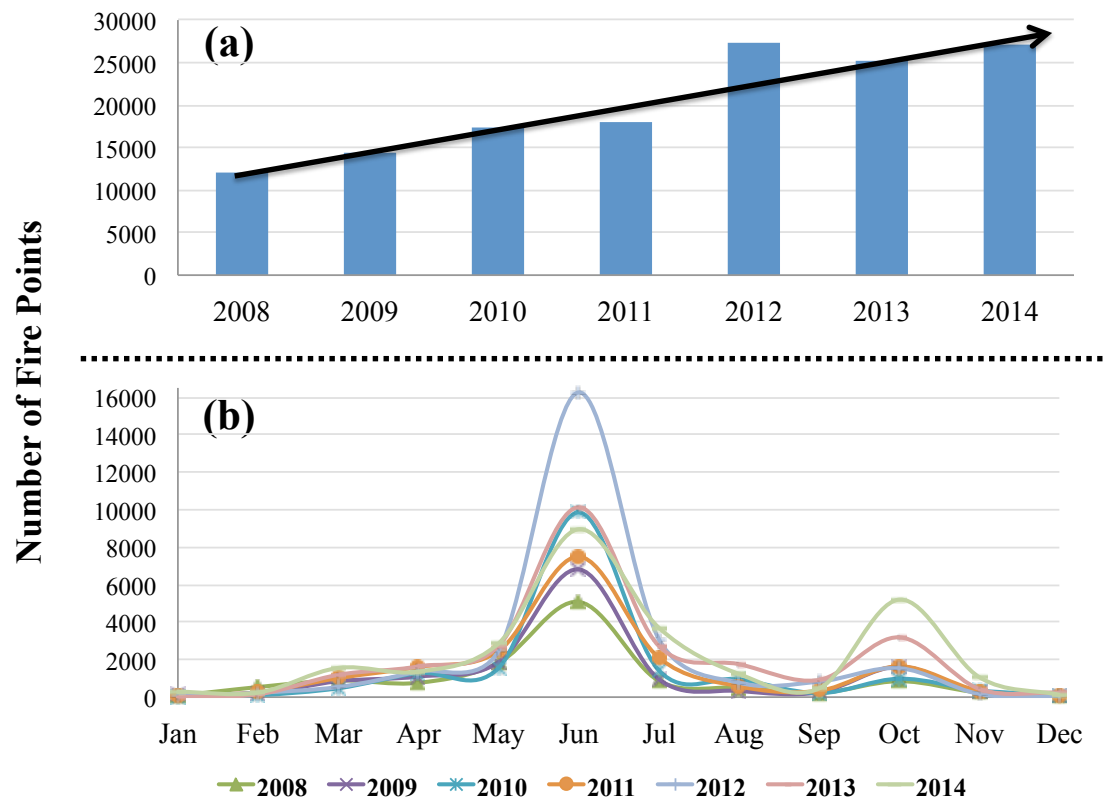


Figure 2

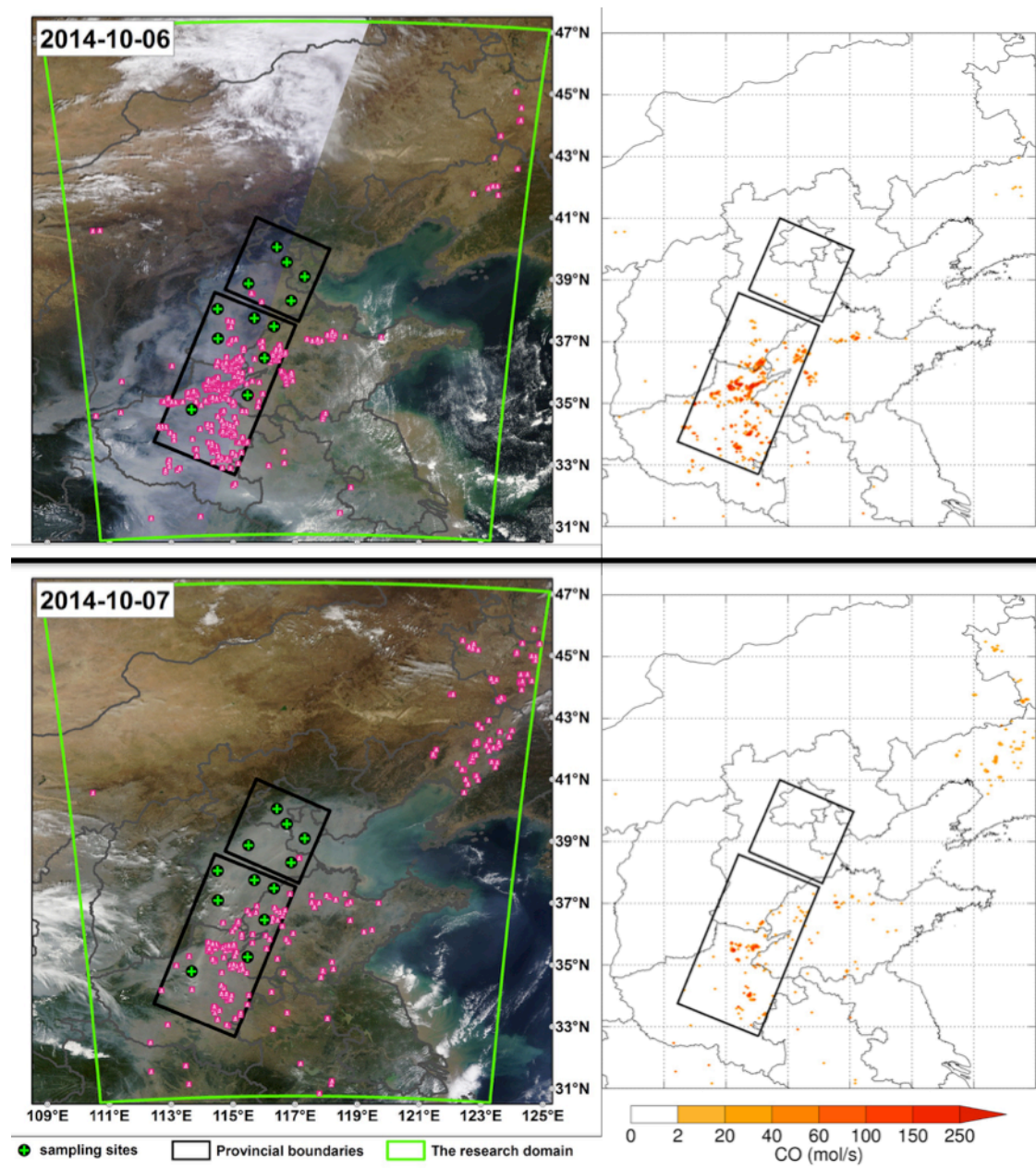


Figure 3

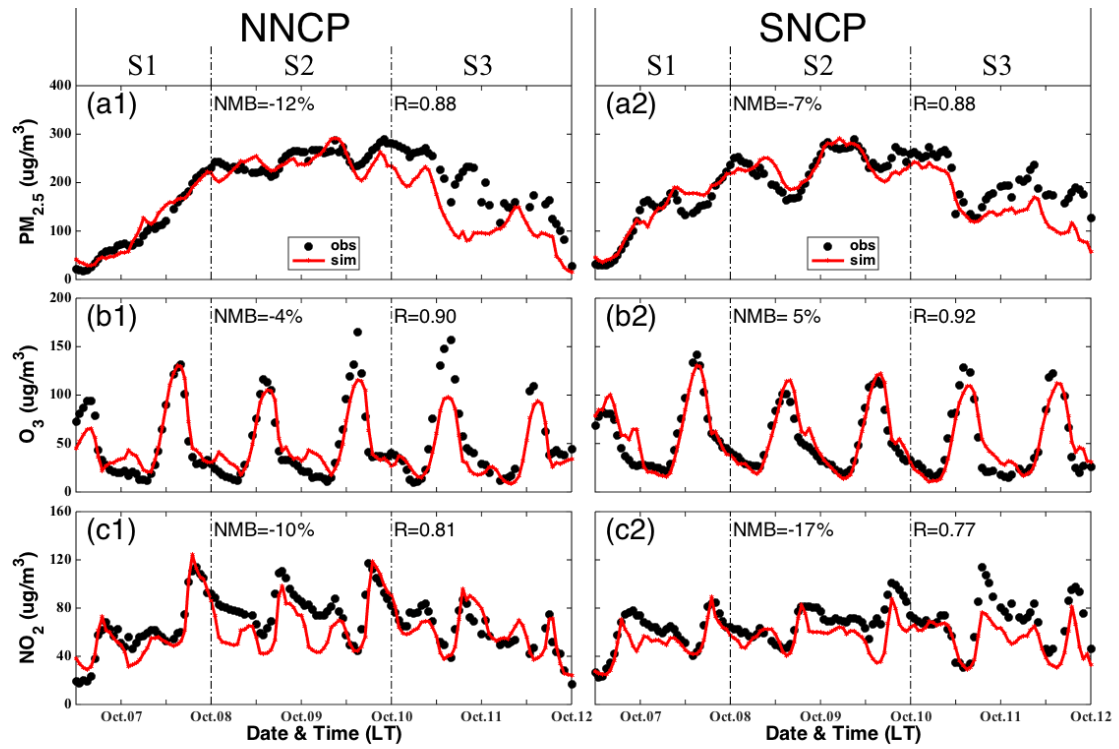


Figure 4

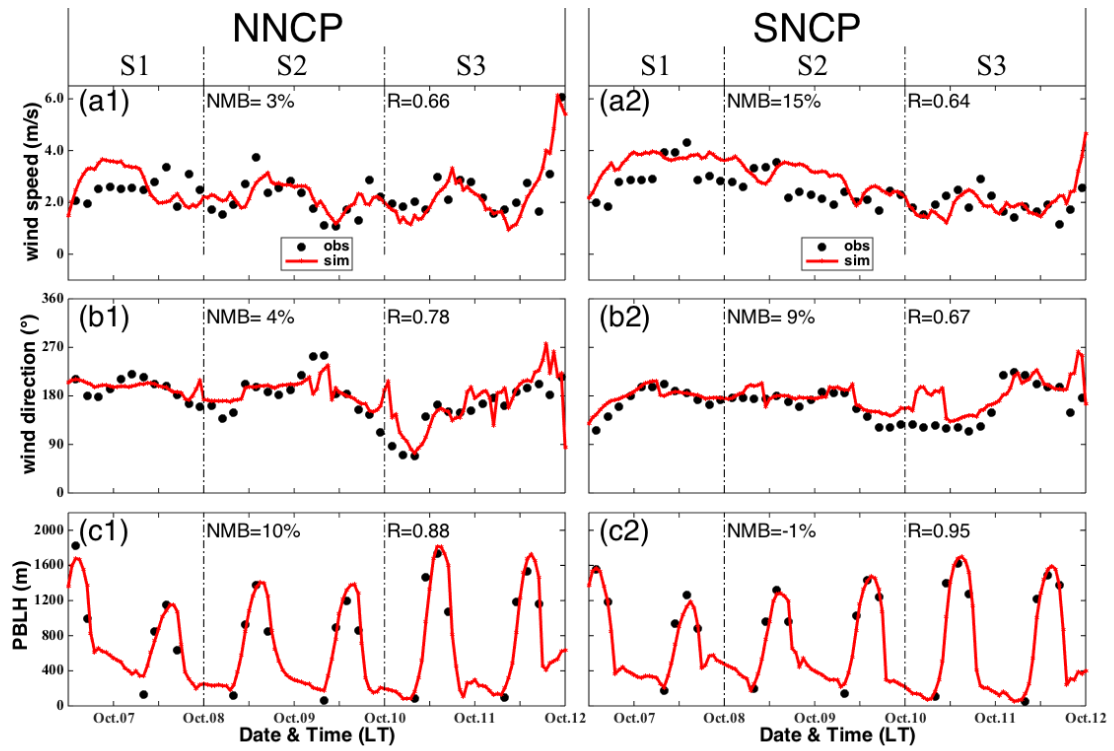


Figure 5

NOAA HYSPLIT MODEL
Backward trajectories ending at 1500 UTC 07 Oct 14
GDAS Meteorological Data

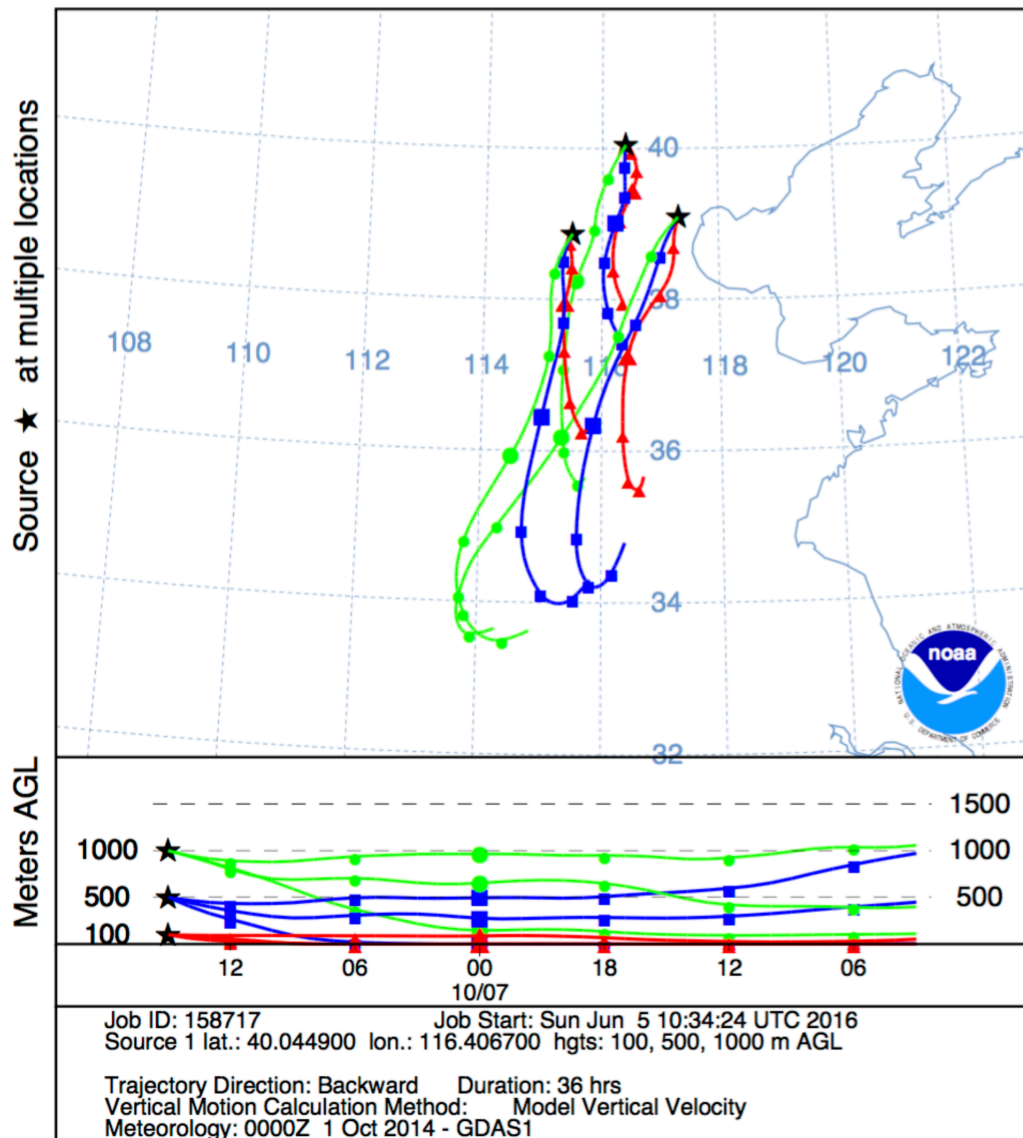


Figure 6

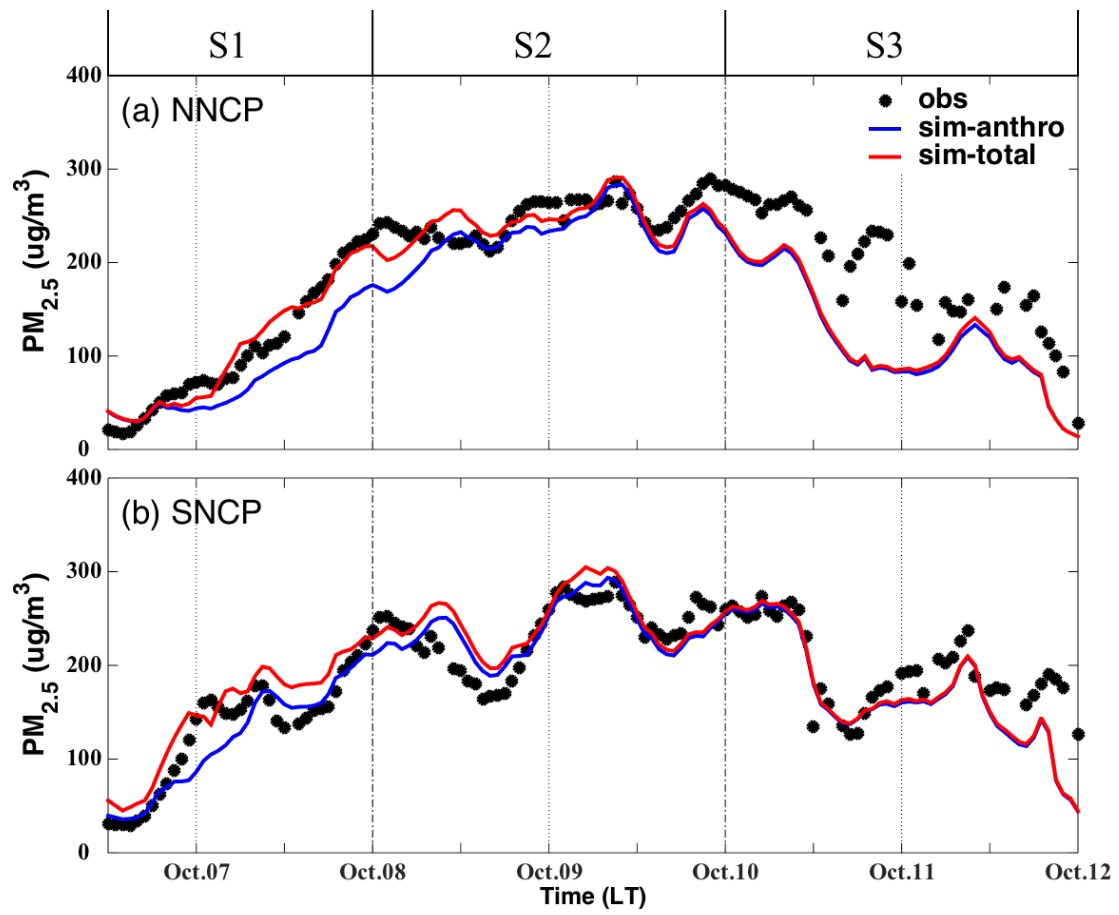


Figure 7

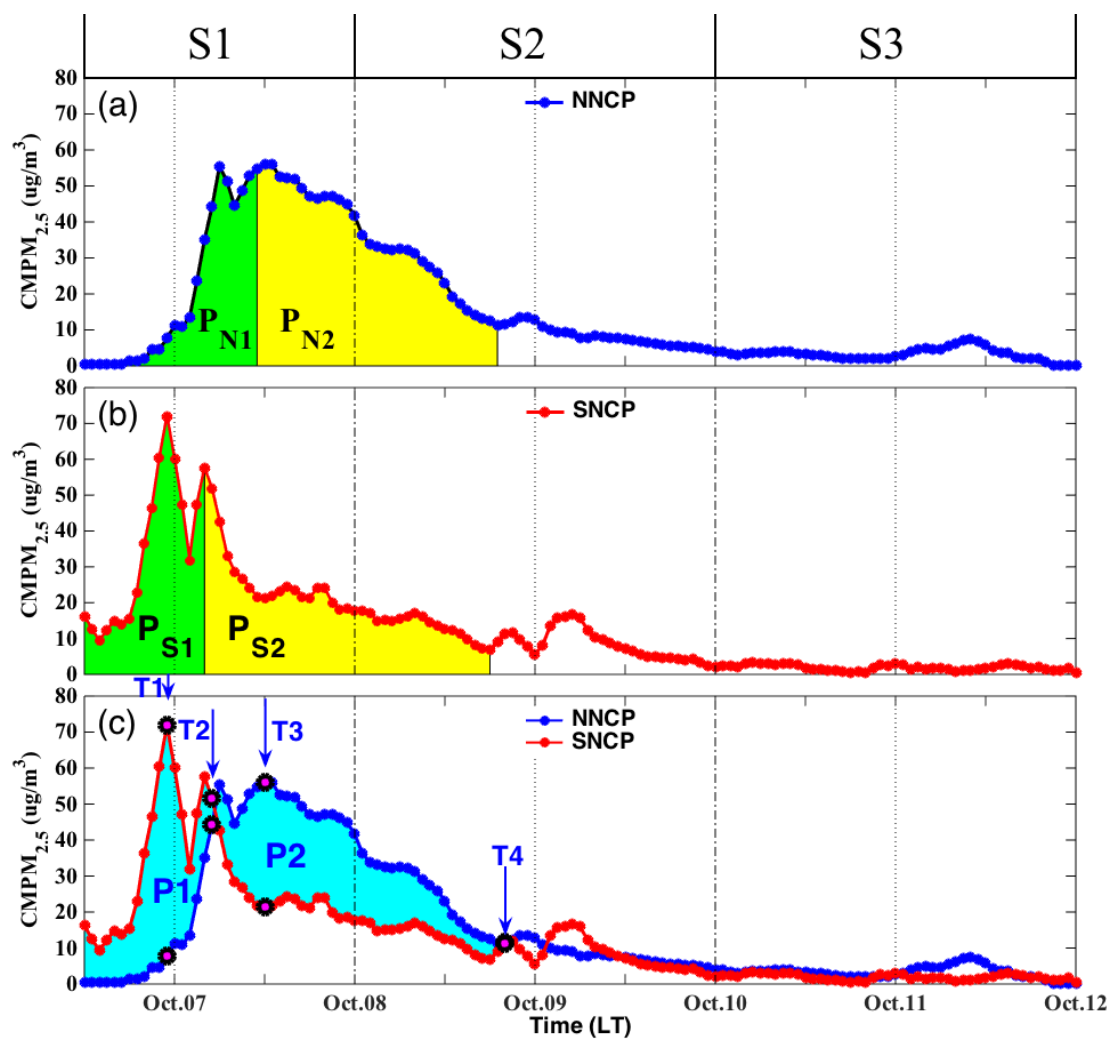
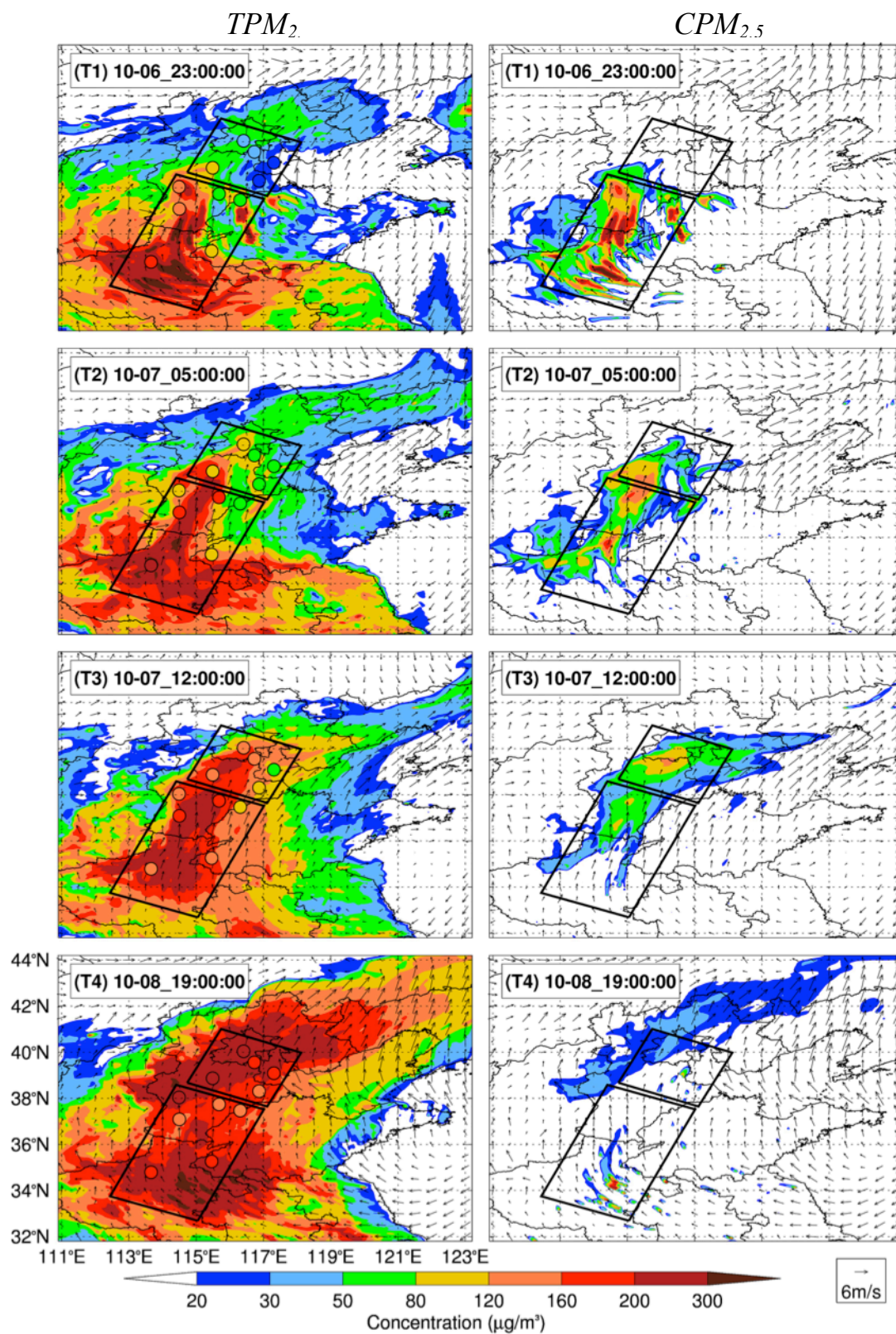


Figure 8

848



849

850

851 Figure 9

852

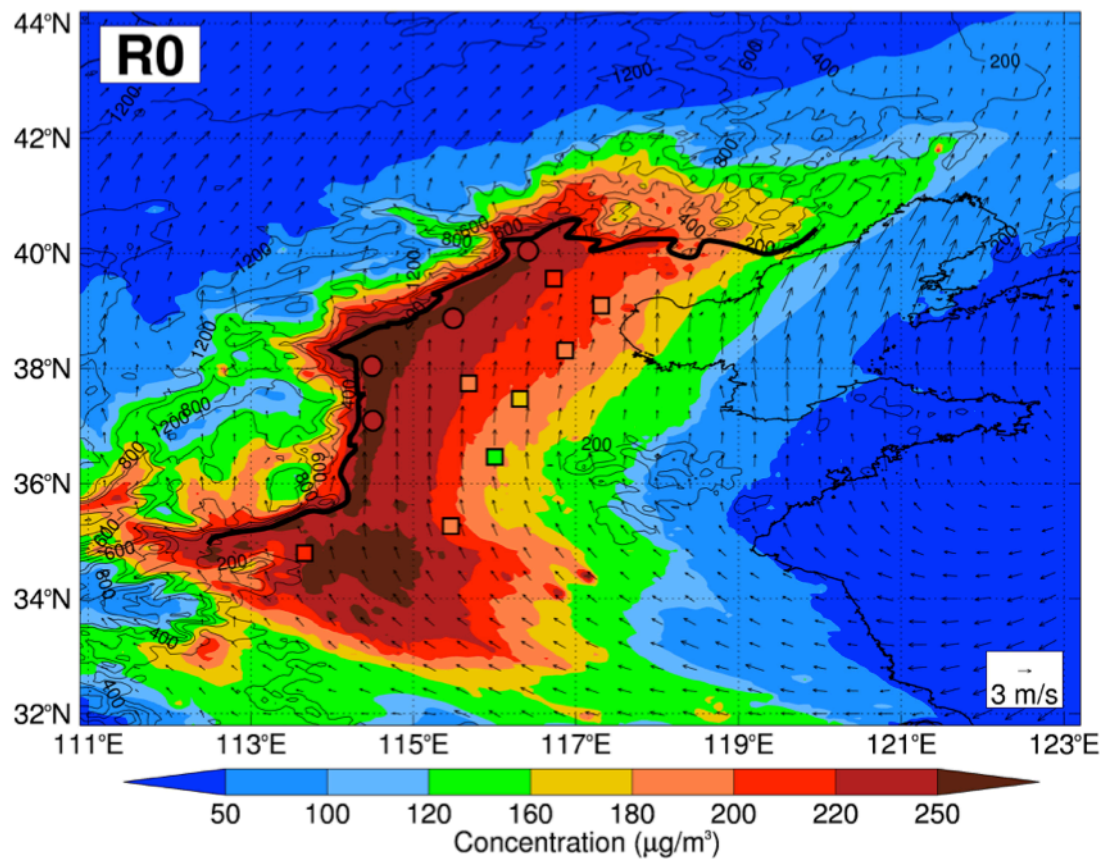


Figure 10

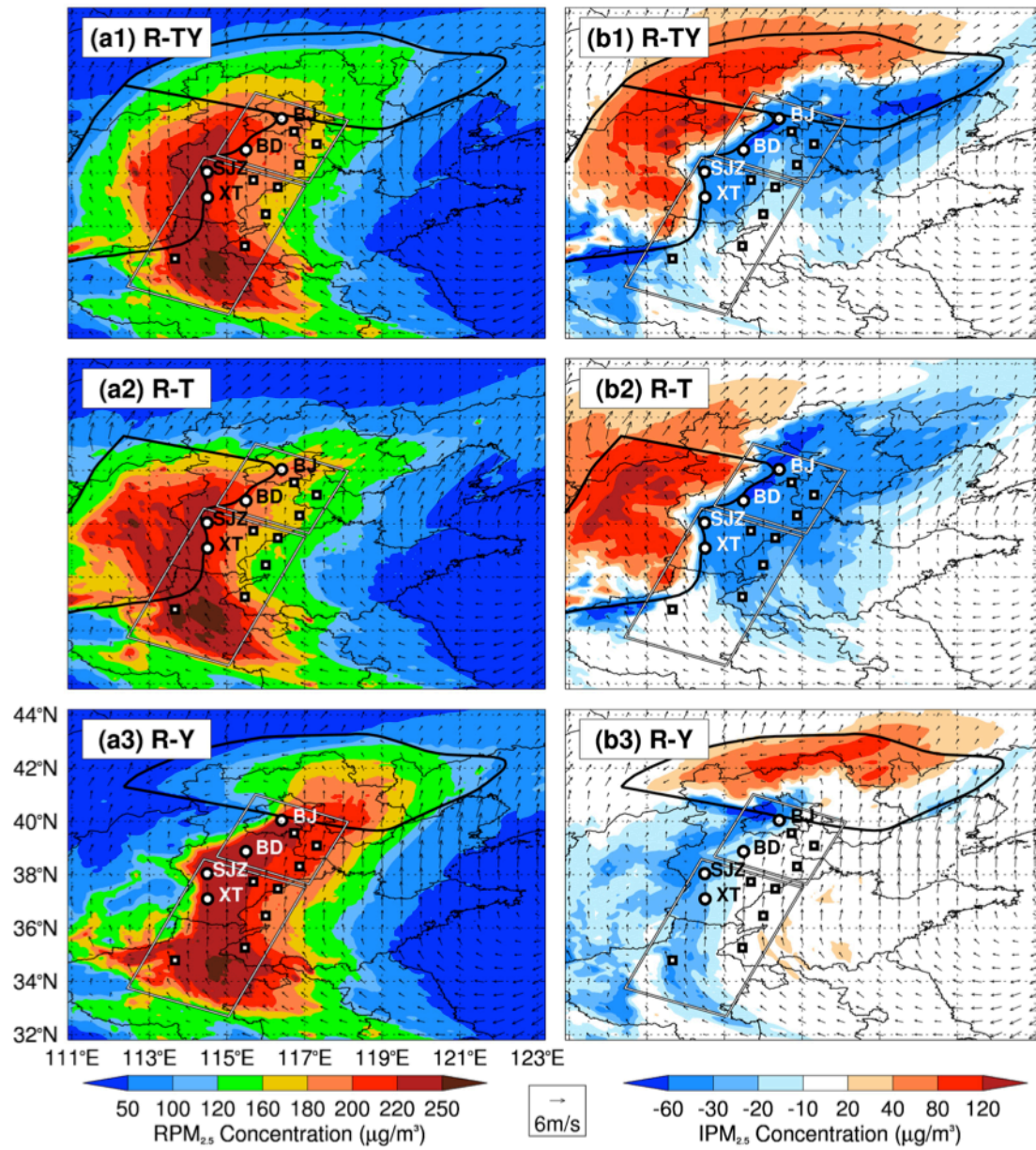


Figure 11